

VOLUME LXXVI

AUG 30 1932

NUMBER 2

# THE ASTROPHYSICAL JOURNAL

AN INTERNATIONAL REVIEW OF SPECTROSCOPY  
AND ASTRONOMICAL PHYSICS

Edited by

GEORGE E. HALE

Mount Wilson Observatory of the Carnegie  
Institution of Washington

HENRY O. GALE

Lysson Physical Laboratory of the  
University of Chicago

EDWIN B. FROST

Yerkes Observatory of the  
University of Chicago

OTTO STRUVE

Yerkes Observatory of the  
University of Chicago

---

SEPTEMBER 1932

|  |                                       |     |
|--|---------------------------------------|-----|
| 17 LEPORIS: A NEW TYPE OF SPECTRUM VARIABLE                            | Olaf Sten                             | 85  |
| THE SURFACE BRIGHTNESS OF THRESHOLD IMAGES                             | Edwin Hubble                          | 100 |
| AN APPLICATION OF THE RADIOMETER: A REGISTERING MICROPHOTOMETER        | Sinclair Smith and Olin C. Wilson Jr. | 117 |
| WIDTH OF THE D LINES OF SODIUM IN ABSORPTION                           | E. A. Kraft                           | 134 |
| THE APPLICATION OF UNSOLD'S CHROMOSPHERIC THEORY TO THE SOLAR<br>LINES | Philip C. Kerman                      | 149 |
| THE EXCITATION OF HELIUM IN THE CHROMOSPHERE                           | Philip C. Kerman                      | 169 |
| A STUDY OF THE COMPOSITE SPECTRUM OF THE A-TYPE STAR 14 COMAE          | W. W. Morgan                          | 184 |

---

THE UNIVERSITY OF CHICAGO PRESS  
CHICAGO, ILLINOIS, U.S.A.

# THE ASTROPHYSICAL JOURNAL

AN INTERNATIONAL REVIEW OF SPECTROSCOPY  
AND ASTRONOMICAL PHYSICS

Edited by

GEORGE E. HALE

Mount Wilson Observatory of the Carnegie  
Institution of Washington

HENRY G. GALE

Ryerson Physical Laboratory of the  
University of Chicago

EDWIN B. FROST

Yerkes Observatory of the  
University of Chicago

OTTO STRUVE

Yerkes Observatory of the  
University of Chicago

WITH THE COLLABORATION OF

WALTER S. ADAMS, Mount Wilson Observatory

JOSEPH S. AMES, Johns Hopkins University

ARISTARCH BELOPOLSKY, Observatoire de Pulkovo

WILLIAM W. CAMPBELL, Lick Observatory

HENRY CREW, Northwestern University

CHARLES FABRY, Université de Paris

ALFRED POWLER, Imperial College, London

EDWIN HUBBLE, Mount Wilson Observatory

HARLOW SHAPLEY, Harvard College Observatory

HEINRICH KAYSER, Universität Bonn

ROBERT A. MILLIKAN, Institute of Technology, Pasadena

HUGH F. NEWALL, Cambridge University

FRIEDRICH PASCHEN, Reichsanstalt, Charlottenburg

HENRY N. RUSSELL, Princeton University

FRANK SCHLESINGER, Yale Observatory

SIR ARTHUR SCHUSTER, Twyford

FREDERICK M. SEARES, Mount Wilson Observatory

The *Astrophysical Journal* is published by the University of Chicago at the University of Chicago Press, 5750 Ellis Avenue, Chicago, Illinois, during each month except February and August. ¶ The subscription price is \$6.00 a year; the price of single copies is 75 cents. Orders for service of less than a half-year will be charged at the single-copy rate. ¶ Postage is prepaid by the publishers on all orders from the United States, Mexico, Cuba, Porto Rico, Panama Canal Zone, Republic of Panama, Dominican Republic, Canary Islands, El Salvador, Argentina, Bolivia, Brazil, Colombia, Chile, Costa Rica, Ecuador, Guatemala, Honduras, Nicaragua, Peru, Hayti, Uruguay, Paraguay, Hawaiian Islands, Philippine Islands, Guam, Samoan Islands, Balearic Islands, Spain, and Venezuela. ¶ Postage is charged extra as follows: for Canada and Newfoundland, 30 cents on annual subscriptions (total \$6.30); on single copies, 3 cents (total 78 cents); for all other countries in the Postal Union, 80 cents on annual subscriptions (total \$6.80), on single copies, 8 cents (total 83 cents). ¶ Patrons are requested to make all remittances payable to The University of Chicago Press, in postal or express money orders or bank drafts.

The following are authorized agents:

For the British Empire, except North America, India, and Australasia: The Cambridge University Press, Fetter Lane, London, E.C. 4. Prices of yearly subscriptions and of single copies may be had on application.

For Japan: The Maruzen Company, Ltd., Tokyo.

For China: The Commercial Press, Ltd., Paoshan Road, Shanghai. Yearly subscriptions, \$6.00; single copies, 75 cents, or their equivalents in Chinese money. Postage extra, on yearly subscriptions 80 cents, on single copies 8 cents.

Claims for missing numbers should be made within the month following the regular month of publication. The publishers expect to supply missing numbers free only when losses have been sustained in transit, and when the reserve stock will permit.

Business correspondence should be addressed to The University of Chicago Press, Chicago, Illinois.

Communications for the editors and manuscripts should be addressed to: Otto Struve, Editor of THE ASTROPHYSICAL JOURNAL, Yerkes Observatory, Williams Bay, Wisconsin.

The cable address is "Observatory, Williamsbay, Wisconsin."

The articles in this journal are indexed in the *International Index to Periodicals*, New York, N.Y.

Applications for permission to quote from this journal should be addressed to The University of Chicago Press, and will be freely granted.

Entered as second-class matter, January 17, 1895, at the Post-Office at Chicago, Ill., under the act of March 5, 1879.

Acceptance for mailing at special rate of postage provided for in Section 1102, Act of October 3, 1917, authorized on July 15, 1918.

PRINTED IN THE U.S.A.

# THE ASTROPHYSICAL JOURNAL

AN INTERNATIONAL REVIEW OF SPECTROSCOPY AND  
ASTRONOMICAL PHYSICS

VOLUME LXXVI

SEPTEMBER 1932

NUMBER 2

## 17 LEPORIS: A NEW TYPE OF SPECTRUM VARIABLE

By OTTO STRUVE

### ABSTRACT

The spectrum of 17 Leporis is composite: the broad hydrogen wings and diffuse  $Mg\ II\ 4481$  constitute the first spectrum, and the sharp lines of  $Fe\ II$ ,  $Ti\ II$ ,  $Fe\ I$ ,  $Sc\ II$ ,  $Cr\ II$ , etc., the second. The radial velocity derived from the first spectrum averages about 0 km/sec.; the second spectrum undergoes large variations in character and velocity. In its normal stage, lasting several months, the second spectrum has strong, sharp lines which give a velocity of about -40 km/sec. At intervals of approximately 155 days the lines of the second spectrum develop violet components which give  $V = -150$  km/sec. These components are first seen in  $Fe\ II$ , then in  $Ti\ II$ , and last of all in  $Sc\ II$ . When the doubling occurs the total intensities of most of the absorption lines are very much reduced. This abnormal stage lasts a few weeks. The cores of the  $H$  lines are strengthened during the abnormal stage, and  $H\beta$  shows a faint emission line on its red side.

During the normal stage the intensities of the absorption lines within any given multiplet show a larger gradient than do the lines of most other stars, for instance,  $\epsilon$  Aurigae and  $\alpha$  Cygni.

The doubling of the lines of the second spectrum and the variations in radial velocity cannot be explained by orbital motion.

It is suggested that the first spectrum is that of the reversing layer, while the second originates in an expanding outer shell of gas. The theoretical contour of the lines and the expected ratio of total absorption to total emission within a line are shown to depend upon the ratio of the radius of the shell to the radius of the star. If we adopt a suitable value for this ratio, we may account for the observed sharpness of the absorption lines and the weakness of the emission lines. The periodic appearance of violet components is attributed to the formation of new shells. A drawback to this hypothesis is the constancy in the light of 17 Leporis.

### I. GENERAL DESCRIPTION OF SPECTRUM

The peculiar variations in the spectrum of 17 Leporis ( $\alpha 6^h 0^m 5;$   
 $\delta -16^\circ 29'$ , Harvard Sp. Ao, ptm. mag. 5.04) have been briefly de-

scribed in an earlier paper.<sup>1</sup> The star has now been observed at the Yerkes Observatory for more than two years, and this discussion is based upon forty-five spectrograms obtained with the Bruce spectrograph attached to the 40-inch refractor.

The normal spectrum of 17 Leporis contains a number of very strong lines of *Fe* II, *Ti* II, and *Sc* II, in addition to strong hydrogen lines, and weak lines of *Fe* I and *Mg* II. The *Henry Draper Catalogue* designates this spectrum as A0, but it is by no means normal; the magnesium line at  $\lambda$  4481 is far too weak for its class and the *Si* II lines  $\lambda$  4128 and  $\lambda$  4131 are not visible on our plates. The strong lines of *Fe* II and *Ti* II, in 17 Leporis, resemble somewhat those in the supergiants  $\epsilon$  Aurigae and  $\alpha$  Cygni. A reproduction of the spectrum of 17 Leporis was published in Volume 72 of this *Journal* (top of Pl. XIV, facing p. 343).

This normal spectrum seems to persist, without any violent changes, for periods of several months. At certain times, however, a series of remarkable changes takes place, the most conspicuous of which is a very marked weakening of the lines of *Fe* II, *Ti* II, *Sc* II, *Fe* I, *Sr* II, *Ca* I, etc. Closer inspection shows that as the lines fade out they are split into two components. The total intensity of the two components is much less than would be expected in a spectroscopic binary. A comparison of 17 Leporis with Mizar shows conclusively that the effect of overlapping of the lines of one component with the continuous spectrum of the other could account for only a small part of the observed decline in intensity. The magnesium line  $\lambda$  4481 does not appreciably change in intensity or in structure, but appears at all times as a faint and diffuse line, suggestive of rapid axial rotation. Contrary to the behavior of the lines of *Fe* II and *Ti* II, the Balmer lines are strengthened when the metallic lines are weakened. The broad hydrogen wings, which are similar to those observed in normal A stars, do not change in appearance. The cores of the Balmer lines, however, which are more or less displaced toward the violet with respect to the wings, undergo large variations in width and intensity. On a few plates there is a faint, rather narrow

<sup>1</sup> *Astrophysical Journal*, 72, 343, 1930; *Publications of the Yerkes Observatory*, 7, Part I, 28, 1929.



TABLE I

17 LEPORIS: 1929 JAN. 2.200

(Reduction to sun, -4.3 km/sec.)

| Line              | Int.  | Meas. Vel.<br>in Km/Sec. | Blends                           | Line                             | Int. | Meas. Vel.<br>in Km/Sec. | Blends       |
|-------------------|-------|--------------------------|----------------------------------|----------------------------------|------|--------------------------|--------------|
| <i>H</i>          |       |                          |                                  | <i>Fe I—Continued</i>            |      |                          |              |
| H $\delta$ .....  | 20    | -64                      | .....                            | 4207.13....                      | 1    | -71                      | .....        |
| H $\gamma$ .....  | 20    | -63                      | .....                            | 4271.70....                      | 1    | 50                       | .....        |
| H $\beta$ .....   | 20    | -77                      | .....                            | 4383.55....                      | 2    | -38                      | .....        |
| H $\beta$ em..... | ..... | +78                      | .....                            | <i>Fe II</i>                     |      |                          |              |
| <i>Ti II</i>      |       |                          |                                  | <i>Si II</i>                     |      |                          |              |
| 4012.40....       | 5     | -34                      | .....                            | 4128.40....                      | 1    | -25                      | .....        |
| 4025.13....       | 2     | 45                       | .....                            | 4173.48....                      | 4    | 54                       | .....        |
| 4053.84....       | 1     | 39                       | .....                            | 4178.87....                      | 4    | 46                       | .....        |
| 4163.65....       | 2     | 55                       | .....                            | 4233.16....                      | 10   | 45                       | .....        |
| 4171.01....       | 2     | 29                       | .....                            | 4296.56....                      | 2    | 31                       | .....        |
| 4200.23....       | 5     | 47                       | .....                            | 4303.18....                      | 3    | 36                       | .....        |
| 4294.10....       | 4     | 34                       | .....                            | 4351.77....                      | 6    | 39                       | .....        |
| 4300.05....       | 7     | 39                       | .....                            | 4385.39....                      | 3    | 46                       | .....        |
| 4302.04....       | 3     | 21                       | <i>Ca I</i>                      | 4491.41....                      | 2    | 49                       | .....        |
| 4307.80....       | 4     | 32                       | .....                            | 4508.29....                      | 4    | 43                       | .....        |
| 4312.88....       | 2     | 32                       | .....                            | 4515.34....                      | 3    | 43                       | .....        |
| 4314.98....       | 4     | 65                       | .....                            | 4520.24....                      | 1    | 32                       | .....        |
| 4337.92....       | 4     | 50                       | .....                            | 4522.64....                      | 4    | 38                       | .....        |
| 4395.04....       | 7     | 44                       | .....                            | 4541.33....                      | 1    | 35                       | .....        |
| 4399.77....       | 2     | 26                       | .....                            | 4555.71....                      | 3    | 46                       | <i>Cr II</i> |
| 4417.53....       | 4     | 48                       | <i>Fe II</i>                     | 4576.31....                      | 1    | 28                       | .....        |
| 4443.80....       | 7     | 39                       | .....                            | 4583.84....                      | 7    | 49                       | .....        |
| 4450.49....       | 1     | 25                       | .....                            | 4629.33....                      | 4    | 58                       | .....        |
| 4464.47....       | 1     | 52                       | .....                            | 4923.92....                      | 7    | -64                      | .....        |
| 4468.49....       | 6     | 44                       | .....                            | <i>Sr II</i>                     |      |                          |              |
| 4488.89....       | 2     | 48                       | <i>Fe II</i>                     | <i>Zr II</i>                     |      |                          |              |
| 4501.27....       | 5     | 42                       | .....                            | <i>Y II</i>                      |      |                          |              |
| 4529.19....       | 1     | 39                       | <i>Fe I</i>                      | <i>Ca I</i>                      |      |                          |              |
| 4533.97....       | 7     | 40                       | .....                            | <i>Fe I</i>                      |      |                          |              |
| 4549.55....       | 12    | 44                       | <i>Fe II</i>                     | 4077.71....                      | 1    | -45                      | .....        |
| 4563.77....       | 4     | 37                       | .....                            | <i>Ti II, <math>\odot</math></i> |      |                          |              |
| 4571.98....       | 5     | 45                       | .....                            | 4161.32....                      | 1    | -70                      | .....        |
| 4580.46....       | 1     | 41                       | .....                            | <i>Fe I</i>                      |      |                          |              |
| 4590.02....       | 1     | 31                       | <i>Cr II</i>                     | 4177.54....                      | 1    | -25                      | .....        |
| 4805.11....       | 1     | -50                      | .....                            | <i>Fe I</i>                      |      |                          |              |
| <i>Fe I</i>       |       |                          |                                  | 4226.80....                      | 3    | -42                      | <i>Fe I</i>  |
| 4045.82....       | 3     | -38                      | .....                            |                                  |      |                          |              |
| 4063.60....       | 1     | 43                       | .....                            |                                  |      |                          |              |
| 4071.75....       | 1     | 30                       | .....                            |                                  |      |                          |              |
| 4132.06....       | 1     | 17                       | .....                            |                                  |      |                          |              |
| 4143.87....       | 1     | 49                       | .....                            |                                  |      |                          |              |
| 4184.33....       | 1     | -39                      | <i>Ti II, <math>\odot</math></i> |                                  |      |                          |              |

TABLE I—*Continued*

| Line         | Int. | Meas. Vel.<br>in Km/Sec. | Blends | Line         | Int. | Meas. Vel.<br>in Km/Sec. | Blends      |
|--------------|------|--------------------------|--------|--------------|------|--------------------------|-------------|
| <i>Cr</i> II |      |                          |        | <i>Sc</i> II |      |                          |             |
| 4242.37....  | 1    | -20                      | .....  | 4246.83....  | 8    | -35                      | .....       |
| 4558.66....  | 3    | 55                       | .....  | 4320.73....  | 2    | 28                       | .....       |
| 4588.21....  | 2    | 39                       | .....  | 4325.36....  | 2    | 28                       | <i>Fe</i> I |
| 4618.82....  | 1    | 20                       | bl     | 4374.73....  | 2    | 46                       | <i>Y</i> II |
| 4824.13....  | 2    | -36                      | .....  | 4415.43....  | 2    | (10)                     | <i>Fe</i> I |
|              |      |                          |        | 4670.47....  | 1    | -44                      | .....       |
|              |      |                          |        | <i>Mg</i> II |      |                          |             |
|              |      |                          |        | 4481.23....  | 3    | +38                      | .....       |

emission line on the red side of the core of  $H\beta$ . The line *Fe* II  $\lambda$  4923 is somewhat abnormal, since it does not vary appreciably in intensity, but remains uniformly strong at all times. A reproduction of the "abnormal" stage of 17 Leporis is shown at the bottom of Plate XIV, Volume 72.

There is no evidence that 17 Leporis may be variable in light. Observations by J. Stebbins with the photo-electric photometer showed no variation over a period of thirty-four days.<sup>1</sup> It is not possible to ascertain whether the star was in its "normal" state throughout the period of the photometric observations of Stebbins. No parallax is available; the proper motion, according to L. Boss,<sup>2</sup> is +0".0002 in  $\alpha$  and +0".001 in  $\delta$ .

## II. THE RADIAL VELOCITIES

Table I is a list of all lines that could be measured on a good plate taken when the star was in its normal stage. The hydrogen lines show a greater velocity of approach than do the lines of other elements; *Ti* II, *Fe* I, *Fe* II, *Sr* II, *Zr* II, *Y* II, *Ca* I, *Cr* II, and *Sc* II give approximately one velocity. The scattering in the radial velocities obtained from lines of any given atom is not entirely due to errors of measurement. Thus, it is certain that the line *Fe* II 4923 gives a systematically greater velocity of approach than do the other

<sup>1</sup> *Publications of the Washburn Observatory*, 15, 75, 1928.

<sup>2</sup> *Preliminary General Catalogue*, No. 1516.

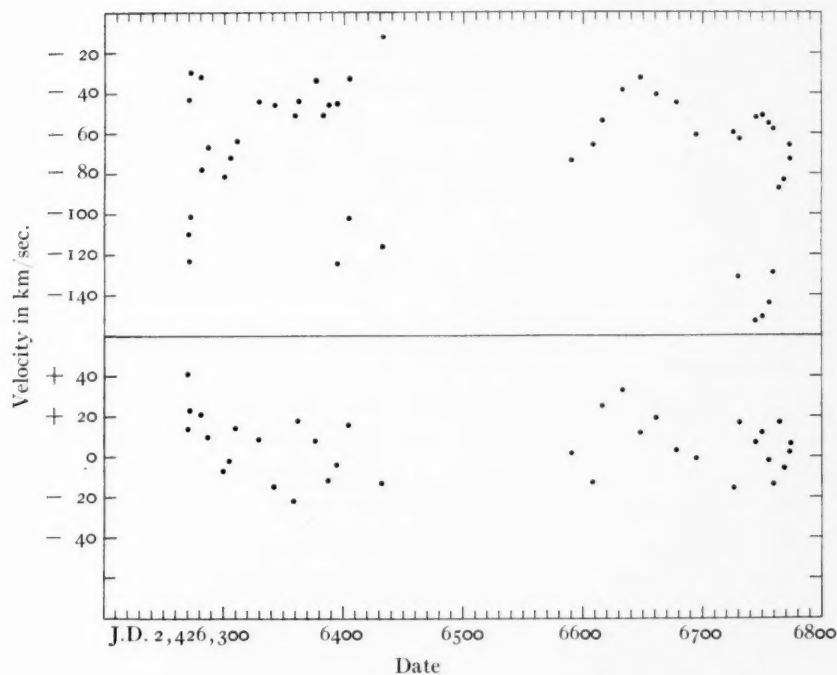


FIG. 1.—Radial velocities of 17 Leporis derived from  $Fe\ II$  lines (top) and  $Mg\ II\ \lambda\ 4481$  (bottom).

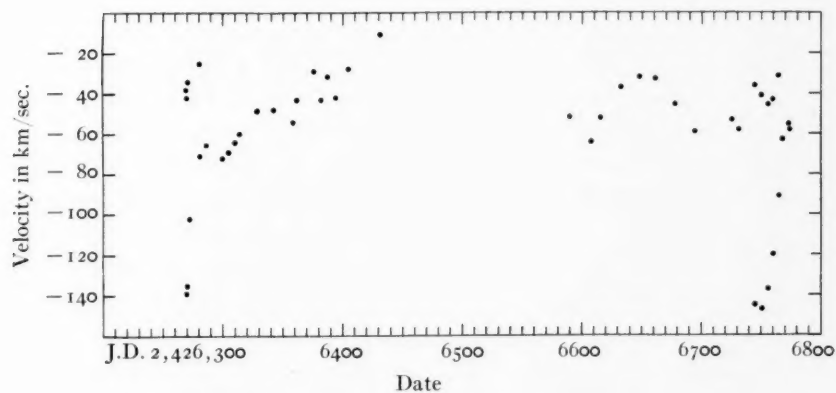


FIG. 2.—Radial velocities of 17 Leporis derived from  $Ti\ II$  lines

*Fe* II lines. The identification of the lines was made with the help of a table recently prepared for the spectrum of  $\gamma$   $\epsilon$  Aurigae.<sup>1</sup>

Table II gives a summary of the measurements of all plates. The velocities obtained from the lines of *Fe* II, *Ti* II, and *Mg* II are plotted in Figures 1 and 2. It is evident that there is no correlation between *Mg* II and the other elements; while the former averages about 0 km/sec., the latter are always negative, rarely exceeding -40 km/sec. The measures of the magnesium line vary between about +40 and -20 km/sec. It is possible that this variation is real, but the line is too diffuse for accurate measurement and no definite conclusion is possible.

The velocity of the other lines varies between about -40 and -150 km/sec. Just before the abnormal stage of spectrum sets in, the stronger *Fe* II lines, particularly  $\lambda$  4233, show a distinct shading toward the violet. In the course of a few weeks this shading becomes more and more conspicuous, until the line is definitely double, with the stronger component at about -40 to -60 km/sec., and the weaker at -120 to -150 km/sec. At the same time the fainter *Fe* II lines also begin to show the doubling, as do also the lines of *Ti* II. The *Sc* II line  $\lambda$  4246, while in the normal stage nearly as strong as *Fe* II  $\lambda$  4233, does not show the effect of doubling until after all lines of *Fe* II and of *Ti* II have become definitely double and weak. Thus, on the plate of October 20, 1930, the violet component of *Sc* II  $\lambda$  4246 is barely visible, while that of *Fe* II  $\lambda$  4233 is relatively very strong.

During the abnormal stage of spectrum the newly formed violet components of the absorption lines gain rapidly in intensity, until the red components have completely faded away. At this stage the lines appear somewhat broad and diffuse, but their intensities are markedly greater than when they are double. The velocity of the single broad lines increases from about -80 km/sec., at first rapidly, and later more slowly, until the normal velocity of about -40 km/sec. is reached. Simultaneously the intensities of the lines increase, and their widths decrease until the normal stage is reached.

The stage of double lines lasts only from two to four weeks, while

<sup>1</sup> E. B. Frost, O. Struve, and C. T. Elvey, *Publications of the Yerkes Observatory*, 7, Part II, 1932. (In press.)



TABLE II\*  
RADIAL VELOCITIES OF 17 LEPORIS

| Date                 | Qual. | H       | Ti II   | Fe II   | Fe I   | Sr II  | Ca II | Ca I   | Cr II  | Sc II  | Mg II  | H $\beta$ em |
|----------------------|-------|---------|---------|---------|--------|--------|-------|--------|--------|--------|--------|--------------|
| 1912 Dec. 6.77.....  | p     | -145(1) | -       | -       | -79(1) | -      | -     | -38(1) | -40(2) | -      | +8(1)  | .....        |
| 1925 Jan. 23.14..... | f     | 84(3)   | 50(12)  | 56(12)  | 52(1)  | .....  | ..... | 38(1)  | 42(2)  | 41(1)  | -4(1)  | .....        |
| 1925 Feb. 1.10.....  | f     | 69(1)   | 28(12)  | 30(10)  | 43(1)  | .....  | ..... | 48(1)  | 42(2)  | 26(1)  | +10(1) | .....        |
| 1928 Dec. 24.25..... | p     | 59(3)   | 37(31)  | 42(21)  | 38(8)  | -34(2) | ..... | 42(1)  | 38(4)  | 36(4)  | -7(1)  | .....        |
| 1928 Dec. 28.19..... | g     | .....   | 35(20)  | 37(15)  | 37(1)  | .....  | ..... | 24(1)  | 40(3)  | 42(2)  | +19(1) | .....        |
| 1929 Jan. 2.20.....  | g     | 72(3)   | 45(30)  | 47(10)  | 46(9)  | 49(1)  | ..... | 46(1)  | 38(5)  | 40(5)  | +34(1) | +74(1)       |
| 1929 Jan. 16.15..... | p     | .....   | 43(9)   | 30(2)   | .....  | .....  | ..... | .....  | .....  | .....  | .....  | .....        |
| 1929 Jan. 30.10..... | g     | 61(3)   | 43(22)  | 45(18)  | 29(2)  | 31(1)  | ..... | 34(1)  | 37(3)  | 40(4)  | -9(1)  | .....        |
| 1930 Oct. 19.40..... | p     | 110(1)  | 130(2)  | 110(1)  | .....  | .....  | ..... | .....  | .....  | .....  | +41(1) | .....        |
| .....                | ..... | .....   | 38(1)   | .....   | .....  | .....  | ..... | .....  | .....  | .....  | .....  | .....        |
| 1930 Oct. 20.44..... | g     | 119(3)  | 135(7)  | 123(7)  | .....  | .....  | ..... | .....  | .....  | 122(1) | +16(1) | 49(1)        |
| .....                | ..... | 41(1)   | 42(10)  | 42(4)   | .....  | .....  | ..... | .....  | .....  | 27(1)  | .....  | .....        |
| 1930 Oct. 22.41..... | g     | 108(3)  | 102(13) | 101(9)  | .....  | .....  | ..... | .....  | 61(1)  | 104(1) | +23(1) | 67(1)        |
| .....                | ..... | .....   | 34(4)   | 30(2)   | .....  | .....  | ..... | .....  | .....  | 26(1)  | .....  | .....        |
| 1930 Oct. 31.40..... | f     | 72(1)   | 71(6)   | 78(8)   | .....  | .....  | ..... | .....  | 76(3)  | .....  | +21(1) | .....        |
| 1930 Nov. 5.40.....  | g     | 79(1)   | 25(4)   | 32(3)   | .....  | .....  | ..... | .....  | 72(2)  | .....  | +10(1) | 35(1)        |
| 1930 Nov. 18.34..... | f     | 96(1)   | 65(10)  | 66(8)   | .....  | .....  | ..... | .....  | 82(2)  | .....  | -7(1)  | .....        |
| 1930 Nov. 23.28..... | p     | .....   | 72(10)  | 81(7)   | .....  | .....  | ..... | .....  | 59(2)  | .....  | -2(1)  | .....        |
| 1930 Nov. 28.20..... | g     | 93(2)   | 69(6)   | 72(6)   | 70(1)  | .....  | ..... | .....  | 76(4)  | 71(1)  | +14(1) | +61(1)       |
| 1930 Dec. 2.26.....  | p     | .....   | 64(21)  | 64(18)  | .....  | .....  | ..... | .....  | .....  | .....  | .....  | .....        |
| 1930 Dec. 17.27..... | g     | 93(1)   | 60(4)   | .....   | .....  | .....  | ..... | .....  | 41(2)  | .....  | +9(1)  | .....        |
| 1930 Dec. 31.25..... | p     | 56(1)   | 48(9)   | 44(9)   | .....  | .....  | ..... | .....  | 43(2)  | .....  | -15(1) | .....        |
| 1931 Jan. 16.13..... | g     | 73(3)   | 48(7)   | 46(6)   | .....  | .....  | ..... | 48(1)  | 61(6)  | 44(5)  | -22(1) | .....        |
| 1931 Jan. 20.23..... | g     | 72(3)   | 54(30)  | 51(20)  | 47(6)  | 54(1)  | ..... | 68(1)  | 43(4)  | 30(2)  | +18(1) | .....        |
| 1931 Feb. 3.22.....  | p     | 68(3)   | 43(10)  | 44(18)  | 51(1)  | -54(1) | ..... | 31(1)  | 26(1)  | 14(2)  | +8(1)  | .....        |
| 1931 Feb. 9.02.....  | p     | .....   | 29(18)  | 34(14)  | 36(1)  | .....  | ..... | .....  | .....  | .....  | .....  | .....        |
| 1931 Feb. 14.03..... | g     | -68(2)  | 43(5)   | 51(1)   | .....  | .....  | ..... | -13(1) | -58(2) | -28(2) | -12(1) | .....        |
| .....                | ..... | .....   | -32(18) | -46(15) | -66(1) | .....  | ..... | .....  | .....  | .....  | .....  | .....        |

\* The radial velocities are given in km/sec. The numbers of lines measured for each atom are shown in parentheses.

TABLE II—Continued

| Date                   | Qual. | H       | Ti II               | Fe II                | Fe I   | Sr II  | Ca II  | Ca I   | Cr II  | Sc II               | M <sub>g</sub> II | H $\beta$ em |
|------------------------|-------|---------|---------------------|----------------------|--------|--------|--------|--------|--------|---------------------|-------------------|--------------|
| 1931 Feb. 21. 07.....  | g     | — 71(3) | — 42(18)            | { -124 (3)<br>45(17) | -43(1) | -64(1) | .....  | -51(1) | -42(3) | - 32(2)             | - 4(1)            | .....        |
| 1931 Mar. 3. 05.....   | g     | 66(3)   | 28(22)              | { 102 (2)<br>33(14)  | -25(2) | 40(1)  | -81(1) | 23(1)  | 57(3)  | { 101(1)<br>- 22(1) | +16(1)            | .....        |
| 1931 Mar. 31. 06.....  | f     | 91(2)   | 11(13)              | { 116 (2)<br>13 (7)  | +10(1) | .....  | .....  | .....  | 27(2)  | + 2(1)              | -13(1)            | .....        |
| 1931 Sept. 6. 43.....  | f     | 87(2)   | 51(12)              | { 74 (9)<br>66(16)   | -24(1) | .....  | .....  | 46(1)  | 55(1)  | - 72(1)             | + 2(1)            | .....        |
| 1931 Sept. 23. 43..... | g     | 92(2)   | 64(20)              | { 74 (9)<br>54(17)   | .....  | .....  | .....  | 57(1)  | 65(2)  | 55(2)               | -13(1)            | .....        |
| 1931 Oct. 1. 43.....   | g     | 69(3)   | 52(23)              | { 37(21)<br>39(17)   | 48(2)  | .....  | .....  | 42(1)  | 56(4)  | 45(2)               | +25(1)            | .....        |
| 1931 Oct. 18. 40.....  | f     | 68(2)   | 37(21)              | { 33(15)<br>41(13)   | 38(1)  | .....  | .....  | 42(1)  | 34(4)  | 34(1)               | +33(1)            | .....        |
| 1931 Nov. 2. 37.....   | f     | 76(2)   | 32(17)              | { 33(15)<br>41(13)   | .....  | .....  | .....  | 50(1)  | 44(4)  | 19(1)               | +12(1)            | .....        |
| 1931 Nov. 16. 30.....  | f     | 62(2)   | 33(14)              | { 41(13)<br>45(15)   | 35(3)  | 24(1)  | .....  | 20(1)  | 47(2)  | 16(1)               | +19(1)            | .....        |
| 1931 Dec. 2. 34.....   | g     | 56(3)   | 45(22)              | { 45(15)<br>61(15)   | .....  | .....  | .....  | 30(1)  | 42(4)  | 41(1)               | + 3(1)            | +72(1)       |
| 1931 Dec. 19. 27.....  | g     | 65(3)   | 59(21)              | { 61(15)<br>60(14)   | 40(2)  | -59(1) | .....  | 69(1)  | 51(5)  | 39(2)               | - 1(1)            | .....        |
| 1932 Jan. 19. 10.....  | g     | 70(3)   | 53(15)              | { 60(14)<br>131 (1)  | 59(1)  | .....  | .....  | 54(1)  | 73(1)  | 47(1)               | -16(1)            | .....        |
| 1932 Jan. 25. 09.....  | f     | 106(3)  | 58(11)              | { 63(11)<br>153 (2)  | .....  | .....  | .....  | 73(1)  | 60(1)  | 41(1)               | +17(1)            | .....        |
| 1932 Feb. 7. 11.....   | f     | 91(2)   | { 144 (3)<br>36 (9) | { 52 (7)<br>151 (2)  | .....  | .....  | .....  | .....  | .....  | 39(1)               | + 7(1)            | .....        |
| 1932 Feb. 13. 04.....  | g     | 104(3)  | { 147 (1)<br>41(14) | { 51(10)<br>144 (3)  | .....  | .....  | .....  | 66(1)  | .....  | 28(1)               | +12(1)            | .....        |
| 1932 Feb. 18. 11.....  | g     | 114(3)  | { 137 (5)<br>46(11) | { 55 (5)<br>129 (3)  | .....  | .....  | .....  | 86(1)  | .....  | { 129(1)<br>23(1)   | - 2(1)            | .....        |
| 1932 Feb. 22. 07.....  | g     | 100(3)  | { 120 (7)<br>43(10) | { 58 (4)<br>87 (7)   | .....  | .....  | .....  | 59(1)  | .....  | { 121(1)<br>29(1)   | -14(1)            | .....        |
| 1932 Feb. 27. 16.....  | f     | 109(2)  | { 90 (7)<br>32 (2)  | .....                | .....  | .....  | .....  | .....  | .....  | 69(1)               | +17(1)            | .....        |
| 1932 Mar. 1. 05.....   | f     | 100(2)  | 63 (8)              | 83 (8)               | .....  | .....  | .....  | .....  | .....  | .....               | - 6(1)            | .....        |
| 1932 Mar. 6. 07.....   | f     | 83(3)   | 55 (9)              | 66 (8)               | .....  | .....  | .....  | .....  | .....  | .....               | + 2(1)            | +75(1)       |
| 1932 Mar. 7. 07.....   | g     | - 85(3) | - 58(11)            | - 73(11)             | -53(1) | .....  | .....  | -66(1) | -60(3) | - 34(1)<br>- 36(1)  | + 6(1)            | .....        |

the normal stage of spectrum may last one hundred days or longer. Whether or not the phenomena are periodic cannot be ascertained from the material available; the abnormal spectrum was observed in October, 1930, and in March, 1932. In March, 1931, there were indications that it was about to set in. It is possible that a period of about one hundred and fifty-five days would satisfy the observations, but there are strong indications that the spectrum was much more abnormal in October, 1930, than in March, 1931; furthermore, the first plate in September, 1931, does not suggest that the star had just been through its abnormal stage.

The hydrogen lines have very strong and broad nuclei during the abnormal stage. On one plate there is a suggestion that  $H\delta$  is double. It is possible that the broadening of the hydrogen lines is caused by the overlapping of two components.

The broad wings of the hydrogen lines are unsymmetrical with respect to the cores. I have extrapolated these wings on a tracing of the plate of January 2, 1929, and measured their center with respect to the narrow core. The result is as shown in the accompanying tabulation:

| Distance between<br>Hydrogen Core and Center of<br>Hydrogen Wings |            |
|---|------------|
| $H\beta$ .....  | 95 km/sec. |
| $H\gamma$ .....   | 92         |
| $H\delta$ .....   | 100        |

The radial velocity obtained from the cores is  $-72$  km/sec. Consequently, the mean velocity from the broad hydrogen wings is  $+24$  km/sec. On the same plate, the magnesium line  $\lambda 4481$  gives  $+34$  km/sec. There can be no doubt that the hydrogen wings and the magnesium line belong together.

It is safe to conclude that in 17 Leporis we are dealing with the superposition of two spectra. The one is a normal A star with considerable rotational broadening; the hydrogen wings and diffuse magnesium  $\lambda 4481$  are the only lines that can be definitely assigned to it. Its radial velocity is something like 0 km/sec. The other spectrum is one of variable lines of  $H$ ,  $Fe$  II,  $Fe$  I,  $Ti$  II,  $Sc$  II,  $Cr$  II, etc., which always give negative velocities.

The weak emission line at  $H\beta$  seems to be strongest during or

shortly following the abnormal stage. Its radial velocity does not appear to vary and the mean is  $+62$  km/sec.

### III. THE SPECTRAL CHANGES

Table III contains a description of the lines on each plate. The changes in intensity and appearance are correlated with the changes in radial velocity. During the abnormal stage the strongest lines of the second spectrum, namely, those of hydrogen, are greatly strengthened; the strongest line of *Fe* II  $\lambda$  4923 remains practically unaltered; rather strong lines (e.g., *Fe* II  $\lambda$  4233) are slightly weakened; average or weak lines fade out almost completely.

TABLE III\*

#### DESCRIPTION OF ABSORPTION LINES OF 17 LEPORIS

|           |   |
|-----------|---|
| 1912 Dec. | 6— <i>Ti</i> II and <i>Fe</i> II faint; possible double; poor plate   |
| 1925 Jan. | 23—All lines sharp and strong; <i>H</i> strong  |
| 1925 Feb. | 1—Same  |
| 1928 Dec. | 24—All lines very narrow and very strong; <i>H</i> strong   |
| 1928 Dec. | 28—Same   |
| 1929 Jan. | 2— <i>Fe</i> II 4233 shows weak violet component; other lines strong and narrow; <i>H</i> strong  |
| 1929 Jan. | 16—Poor plate   |
| 1929 Jan. | 30—Lines strong, but slightly broadened; <i>H</i> strong  |
| 1930 Oct. | 19—Poor plate   |
| 1930 Oct. | 20—All lines very weak and double; <i>Ti</i> II lines have components of equal strength; <i>Fe</i> II 4233 has stronger component on violet side; <i>Sc</i> II 4246 has strong red component and extremely weak violet component; <i>H</i> strong |
| 1930 Oct. | 22—Violet component of <i>Fe</i> II much strengthened; <i>Sc</i> II 4246 has stronger component on red side; but violet component is well visible; <i>Ti</i> II lines have slightly stronger violet components                                    |
| 1930 Oct. | 31—Violet components of double lines much stronger than red components  |
| 1930 Nov. | 5—Lines single, broad; intensity of lines greater than on preceding four plates   |
| 1930 Nov. | 18—Same   |
| 1930 Nov. | 23—Poor plate   |
| 1930 Nov. | 28—Lines rather strong, and but slightly broadened  |
| 1930 Dec. | 2—Poor plate  |
| 1930 Dec. | 17—Lines very strong and rather narrow; slightly shaded toward violet   |
| 1930 Dec. | 31—Lines strong, narrow, symmetrical  |



TABLE III—Continued

- 1931 Jan. 16—Lines very strong and narrow; *H* relatively weak; a few lines (*Mg* II 4481, *Fe* I 4045, *Sr* II 4215, etc.), look broad and diffuse on this and on other plates
- 1931 Jan. 20—Same
- 1931 Feb. 3—Same
- 1931 Feb. 9—Poor plate
- 1931 Feb. 14—*Ti* II lines narrow and sharp; *Fe* II shaded toward violet; *Sc* II 4246 very narrow and sharp
- 1931 Feb. 21—*Fe* II has faint violet components; *Ti* II lines slightly broadened, but strong; *H* strong
- 1931 Mar. 3—*Fe* II has violet components; *Ti* II broadened; *H* very strong
- 1931 Mar. 31—Same
- 1931 Sept. 6—Lines narrow, strong
- 1931 Sept. 23—Lines very narrow, very strong; *H* relatively weak
- 1931 Oct. 1—Same
- 1931 Oct. 18—Same
- 1931 Nov. 2—Lines slightly shaded toward violet
- 1931 Nov. 16—Lines appreciably broadened; *H* relatively strong
- 1931 Dec. 2—Lines rather narrow and strong; *H* strong
- 1931 Dec. 19—Same, but *Mg* II very strong and very broad with diffuse edges
- 1932 Jan. 19—*Fe* II shaded toward violet; *Ti* II slightly broadened; *H* strong
- 1932 Jan. 25—Shading of *Fe* II lines more pronounced, and some *Fe* II lines are double, with weak violet components; *Ti* II broadened; *Sc* II 4246 relatively narrow; *H* strong
- 1932 Feb. 7—*Fe* II definitely double, with stronger components on red side; *Ti* II shows extremely weak violet components
- 1932 Feb. 13—Same
- 1932 Feb. 18—Lines very weak and double; resembles plate of October 20, 1930; *H* very strong
- 1932 Feb. 22—Same; red components of all lines stronger than violet components
- 1932 Feb. 27—Lines slightly stronger; doubling less pronounced, especially in *Fe* II lines, which are broad; *Ti* II has stronger components on violet side; *H* strong
- 1932 Mar. 1—Lines broad, but not definitely double
- 1932 Mar. 6—Same
- 1932 Mar. 7—Lines not so broad and not quite so weak; *H* strong

\* The descriptions refer to the lines of *Ti* II and *Fe* II unless otherwise specified.

#### IV. INTENSITIES OF ABSORPTION LINES

Plate XI shows the spectra of 17 Leporis and  $\epsilon$  Aurigae. It is immediately noticeable that while many of the strong lines are of about

equal intensity in the two stars, the faint lines are almost entirely missing in  $\epsilon$  Leporis. A careful study of various multiplets of  $Fe\ II$  and  $Ti\ II$  (some of which are marked on the plate) shows conclusively that the relative intensities within any one multiplet are

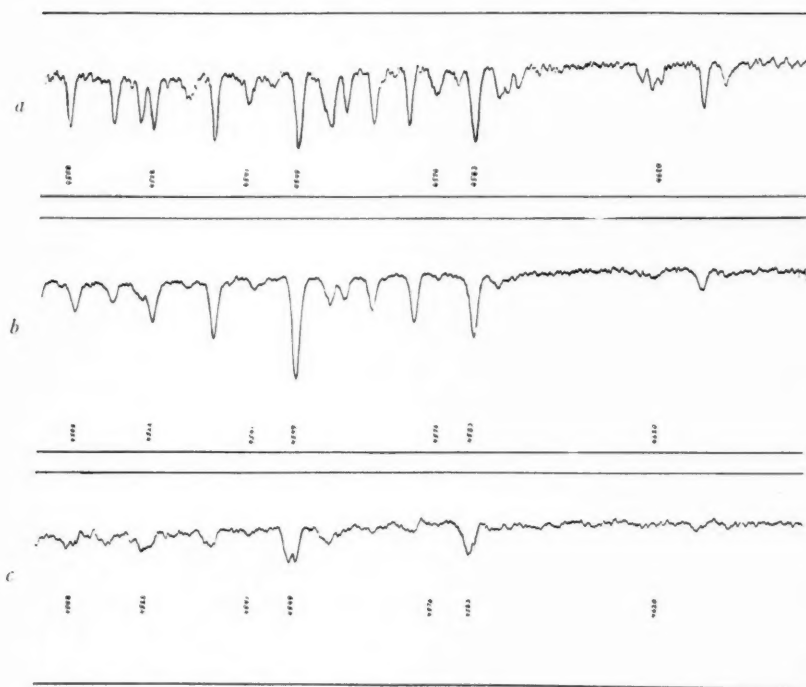


FIG. 3.—Microphotometer tracings of (a)  $7\epsilon$  Aurigae; (b)  $17$  Leporis in normal stage; (c)  $17$  Leporis in abnormal stage.

not the same in the two stars. In all cases the ratio, strong line/weak line, is much greater for  $17$  Leporis than for  $\epsilon$  Aurigae (Fig. 3).

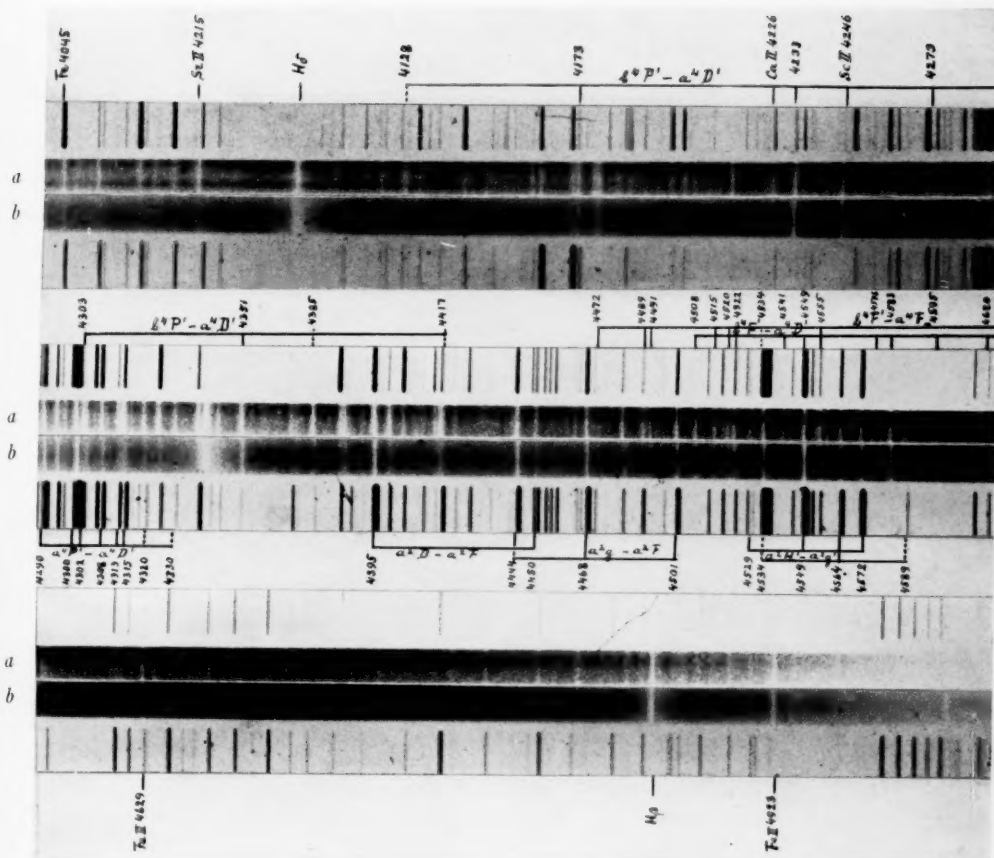
I have accurately measured with the microphotometer the members of the multiplet  $b^4F' - a^4D'$  of  $Fe\ II$ . (The designations in Plate XI are those given by H. N. Russell<sup>1</sup> in his papers of 1926 and 1927; the new multiplet designations may be conveniently taken from a recent paper by Miss C. Moore.)<sup>2</sup> The computed intensities resulting from the well-known formulae of Russell<sup>3</sup> are given in the third line

<sup>1</sup> *Astrophysical Journal*, **64**, 194, 1926; **66**, 283, 1927.

<sup>2</sup> *Ibid.*, **75**, 238, 1932.

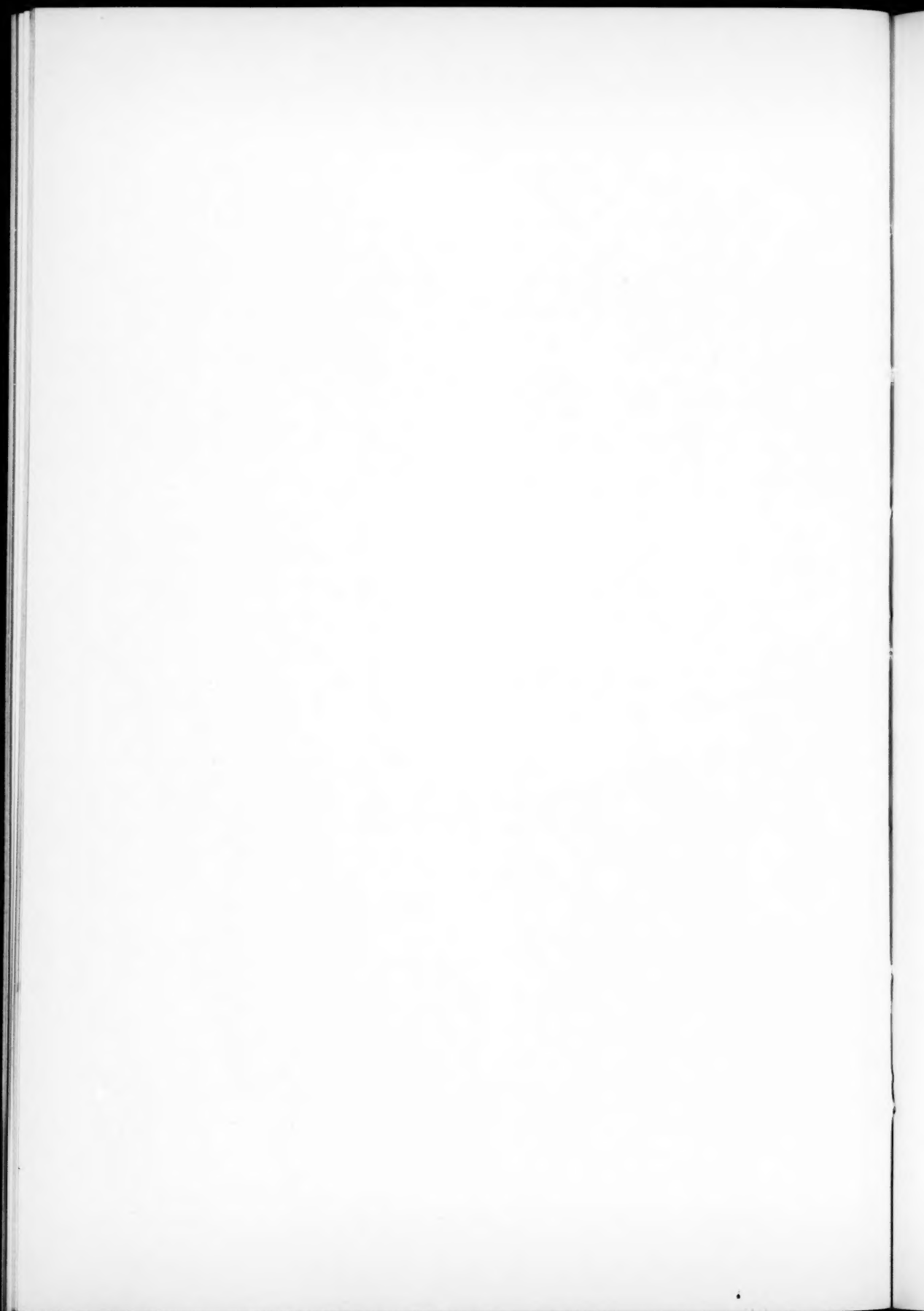
<sup>3</sup> *Proceedings of the National Academy of Sciences*, **11**, 314 and 322, 1925.

# PLATE XI



Spectra of 7ε Aurigae (a) and 17 Leporis (b); the multiplets indicated at the top of each strip are due to Fe II; those at the bottom belong to Ti II. (The line Ca I 4226 is incorrectly assigned to Ca II in the reproduction.)







of Table IV. The total absorbed energies, should, in the case of radiation damping, be proportional to the square roots of the multiplet intensities,<sup>1</sup> which are given in the fourth line. The observed total absorbed energies for  $\epsilon$  Aurigae and for 17 Leporis are given in the fifth and sixth lines. The units were chosen in such a way that the sum of all intensities within the multiplet is 100. The ratio  $\epsilon$  Aurigae/17 Leporis was taken from the original measurements before the arbitrary units mentioned above had been introduced.

It will be noticed that in  $\epsilon$  Aurigae the decline in intensity within the multiplet is slower than that predicted by the square-root law, while in 17 Leporis it is faster—not as fast, however, as in emission.

TABLE IV  
INTENSITIES OF ABSORPTION LINES

| Line Designation             | $\frac{4583}{bF_5'-aD_4'}$ | $\frac{4540}{F_4'-D_3'}$ | $\frac{4522}{F_3'-D_2'}$ | $\frac{4508}{F_2'-D_1'}$ | $\frac{4620}{F_4'-D_4'}$ | $\frac{4576}{F_3'-D_3'}$ | $\frac{4541}{F_2'-D_2'}$ |
|------------------------------|----------------------------|--------------------------|--------------------------|--------------------------|--------------------------|--------------------------|--------------------------|
| Comp. int. ....              | 36                         | 25                       | 16                       | 10                       | 4                        | 5                        | 4                        |
| V Comp. int. ....            | 25                         | 20                       | 16                       | 13                       | 8                        | 9                        | 8                        |
| $\epsilon$ Aurigae. ....     | 22                         | 19                       | 15                       | 13                       | 8                        | 12                       | 11                       |
| 17 Leporis. ....             | 26                         | 27                       | 19                       | 13                       | 5                        | 4                        | 7                        |
| $\epsilon$ Aur./17 Lep. .... | 1.14                       | 0.93                     | 1.07                     | 1.30                     | 1.88                     | 4.35                     | 2.22                     |

It is difficult to interpret this result theoretically. For radiation damping

$$E_{\text{abs}} \propto \sqrt{I_{\text{em}}}.$$

If the lines are greatly broadened by thermal Doppler effect, we have<sup>1</sup>

$$E_{\text{abs}} \propto I_{\text{em}}.$$

This would tend to produce an effect in the desired direction. There is, however, no reason to believe that any very pronounced thermal Doppler effect is present. Although 17 Leporis is somewhat earlier in spectral class than  $\epsilon$  Aurigae, there are many stars of the same spectral class as 17 Leporis, or earlier, in which the relative intensities are similar to those in  $\epsilon$  Aurigae. The peculiarity in 17 Leporis is, therefore, not caused by temperature.

If the hypothesis proposed in section vi holds, it may be that the

<sup>1</sup> Struve and Elvey, *Astrophysical Journal*, 72, 267, 1930.

velocities in the shell have a greater dispersion than would be expected from the spectral type. This could not, however, be reconciled with the extreme sharpness of the lines in the normal stage.

I do not know of any other star that shows the same phenomenon, and it may be limited to such peculiar objects as 17 Leporis. But the fact that the relative intensities within a multiplet may not always be the same in all stars would seriously affect conclusions based upon calibrations of intensity estimates made for a single spectrum.

It should be noted that the rapid gradient of the intensities in 17 Leporis is present in nearly all the elements. The ratio of the strongest line of one multiplet of *Fe* II to the strongest line of another is subject to the same effect. All lines that are normally strong in A-type stars (with the exceptions mentioned above) are also strong in 17 Leporis. But the fainter lines are either extremely weak or entirely absent in the latter.

#### V. BINARY HYPOTHESIS

In nearly all cases heretofore investigated double absorption lines in stellar spectra have been satisfactorily explained by orbital motion. It is, therefore, appropriate to determine whether the changes in the radial velocities of 17 Leporis may be attributed to the same cause.

Referring to Table II and to Figures 1 and 2, we find that when the duplicities are first observed the velocity obtained from the principal component is between  $-40$  and  $-60$  km/sec. But the same velocity is obtained when the lines are perfectly sharp and single. This rules out the binary hypothesis. It is also of interest to note that the duplicity always begins with the formation of a weak violet component which rapidly gains in strength. Faint components have in no case been observed on the red side of the principal lines.

The difference between the velocities of *Mg* II  $\lambda$  4481 and the hydrogen wings on one side, and the strong lines of *Fe* II, *Ti* II, *H*, etc., on the other, is not caused by orbital motion. It is, of course, possible, though not probable, that we are dealing with a composite spectrum of an optical double, or of a physical binary in slow relative orbital motion. In the latter case, however, the large negative velocity of the strong metallic lines would remain unexplained.

## VI. PROPOSED HYPOTHESIS

The large negative velocity of the hydrogen cores and the occasional appearance of emission on the red side of  $H\beta$  suggest a certain similarity to P Cygni. If, for the latter star, we are willing to accept the hypothesis of an expanding shell of gas,<sup>1</sup> it is reasonable to consider a similar hypothesis for 17 Leporis. In that case the narrow lines of  $Fe\ II$ ,  $Ti\ II$ , etc., would also be attributed to the shell. That these are not accompanied by emission would not be contrary to the observed evidence in P Cygni; in the latter I have measured many lines belonging to  $O\ II$  and to other elements which show no emission.

The similarity between P Cygni and 17 Leporis extends still farther. In both the  $H$  lines show a greater velocity of approach than the lines of other elements. Table V gives a summary of my measurements of a recent spectrogram of P Cygni.

The state of excitation of the two shells is, of course, not the same. That of P Cygni corresponds to a star of class B2. The spectrum 17 Leporis has been classified as A0, but the faintness of  $Mg\ II\ \lambda\ 4481$  and the great intensity of  $Fe\ II$ ,  $Ti\ II$ ,  $Sc\ II$ , etc., make it difficult to assign a spectral class to its shell.

In P Cygni all lines (excepting interstellar H and K) show large negative displacements, and are therefore to be attributed to the shell; the spectrum of the reversing layer is not present. In 17 Leporis the spectrum of the reversing layer is shown by  $Mg\ II\ \lambda\ 4481$  (which is missing in the spectrum of the shell) and by the wings of the Balmer lines.

The theoretical contour of an absorption line produced by an expanding atmosphere has been derived by H. Shapley and S. B. Nicholson.<sup>2</sup> If  $\theta$  is the angle between the line of sight and the line joining the center of the star with any given point in the reversing layer, we have

$$V = \cos \theta ; dV = -\sin \theta d\theta .$$

Consider a uniformly bright stellar disk. All points at an apparent distance  $r = \sin \theta$  from the center have the same radial component

<sup>1</sup> J. Halm, *Proceedings of the Royal Society of Edinburgh*, **25**, 513, 1904; C. S. Beals, *Publications of the Dominion Astrophysical Observatory, Victoria*, **4**, 271, 1930; *Monthly Notices of the Royal Astronomical Society*, **91**, 966, 1931.

<sup>2</sup> *Proceedings of the National Academy of Sciences*, **5**, 417, 1919.

TABLE V  
RADIAL VELOCITIES OF P CYGNI: 1931 SEPT. 12. 25  
(Reduced to the sun)

| LINE             | ABSORPTION |      | EMISSION |      | LINE                | ABSORPTION |      | EMISSION |      |
|------------------|------------|------|----------|------|---------------------|------------|------|----------|------|
|                  | Int.       | Vel. | Int.     | Vel. |                     | Int.       | Vel. | Int.     | Vel. |
| H $\delta$ ..... | 10         | -185 | 10       | -42  |                     |            |      |          |      |
| H $\gamma$ ..... | 10         | -192 | 10       | -12  |                     |            |      |          |      |
| <i>He I</i>      |            |      |          |      |                     |            |      |          |      |
| 4120.81....      | 4          | -98  | 4        | +5   | 4241.80....         | 2          | -161 |          |      |
| 4143.77....      | 5          | 107  | 5        | +2   | 4426.05....         | 1          | 91   |          |      |
| 4387.93....      | 6          | 119  | 5        | -1   | 4447.04....         | 2          | 130  | 2        | -9   |
| 4437.55....      | 2          | 104  | 1        | -6   | 4506.50....         | 1          | 123  |          |      |
| 4471.48....      | 10         | -161 | 10       | -11  | 4601.49....         | 4          | 94   | 4        | -13  |
| <i>He II</i>     |            |      |          |      | 4607.17....         | 4          | 89   | 4        | +10  |
|                  |            |      |          |      | 4613.88....         | 3          | 88   | 3        | +27  |
| 4685.81....      | 1          | -118 |          |      | 4621.30....         | 4          | 101  | 3        | +7   |
| <i>O II</i>      |            |      |          |      | 4630.55....         | 6          | 100  | 5        | +15  |
| 4069.80....      | 2          | -84  |          |      | 4643.15....         | 7          | -115 | 5        | +4   |
| 4072.16....      | 1          | 38   |          |      | <i>N III</i>        |            |      |          |      |
| 4075.87....      | 1          | 63   |          |      | 4097.31....         | 1          | -93  | 2        | +25  |
| 4253.98....      | 4          | 112  |          |      | 4510.92....         | 1          | -79  |          |      |
| 4317.16....      | 2          | 112  |          |      | <i>C II</i>         |            |      |          |      |
| 4319.65....      | 2          | 84   |          |      | 4267.27....         | 1          | -130 | 1        | -34  |
| 4345.57....      | 3          | 82   |          |      | <i>Mg II</i>        |            |      |          |      |
| 4349.44....      | 4          | 83   |          |      | 4481.23....         | 2          | -119 | 1        | -3   |
| 4366.91....      | 2          | 72   | 1        | +30  | <i>S III?</i>       |            |      |          |      |
| 4414.89....      | 2          | 81   | 2        | +11  | 4285.00....         | 2          | -101 |          |      |
| 4590.98....      | 1          | 70   |          |      | Unidentified Lines* |            |      |          |      |
| 4596.19....      | 1          | 88   |          |      | 4382.43....         | 2          | -147 | 3        | +17  |
| 4649.15....      | 6          | 67   |          |      | 4395.95....         | 3          | 141  | 3        | -38  |
| 4661.65....      | 2          | -62  |          |      | 4419.62....         | 4          | 158  | 4        | -26  |
| <i>Si III</i>    |            |      |          |      | 4431.03....         | 4          | -160 | 3        | -30  |
| 4552.65....      | 5          | -92  | 2        | +0   |                     |            |      |          |      |
| 4567.87....      | 4          | 104  |          |      |                     |            |      |          |      |
| 4574.78....      | 3          | -96  |          |      |                     |            |      |          |      |
| <i>Si IV</i>     |            |      |          |      |                     |            |      |          |      |
| 4088.86....      | 3          | -61  |          |      |                     |            |      |          |      |
| 4116.10....      | 3          | -42  | 1        | +47  |                     |            |      |          |      |

\* The wave-lengths of these lines were taken from: O. Struve, *Astrophysical Journal*, 74, 225, 1931. The line  $\lambda$  4396 may be due to O II but its emission appears too strong.



of the velocity of expansion. Any given radial velocity  $0 \leq V \leq V_0$  will be observed from a portion of the area of the disk proportional to

$$2\pi r dr = 2\pi \sin \theta \cos \theta d\theta = -2\pi V dV.$$

Since for small intervals of  $\lambda$

$$dV \propto d\lambda,$$

the contour of the absorption line is simply a straight line:

$$I = \text{Const. } V = \text{Const. } (\lambda - \lambda_0).$$

This equation agrees with the one derived by Shapley and Nicholson, and has been applied by them to the spectra of pulsating stars.

In the case of 17 Leporis,  $V_0$  is at least 100 km/sec., and the lines should therefore show an appreciable amount of unsymmetrical broadening. This is not observed, and we may therefore conclude that the expanding shell is not identical with the reversing layer.

If the shell is outside the star at a distance  $d$  from the center, we derive exactly the same expression:

$$r = d \sin \varphi; dr = d \cos \varphi d\varphi; V = \cos \varphi; dV = -\sin \varphi d\varphi.$$

Consequently

$$2\pi r dr = -2\pi d^2 V dV$$

and

$$I = \text{Const. } V = \text{Const. } (\lambda - \lambda_0).$$

But while in the case of an expanding reversing layer  $V$  varies all the way from  $V_0$  to zero, the limits for the distant shell are  $V_0$  and  $V_0 \sqrt{1 - (R^2/d^2)}$ , where  $R$  is the radius of the star. It is evident that even for a shell comparatively close to the surface of the star, the line will be relatively narrow. Thus, for  $R/d = \frac{1}{2}$  the total width of the line would be reduced to 0.14 of the value which would apply to an expanding atmosphere at  $d = R$  (Fig. 4). It is clear that the narrow absorption lines in 17 Leporis at normal stage agree well with the proposed hypothesis. With our dispersion it is impossible to test whether the bottom of the absorption lines actually presents the

asymmetry required by the simple linear formula. It is, of course, to be expected that the darkening toward the limb will change the contour somewhat.<sup>1</sup>

It remains to be seen whether the absence of appreciable emission in the metallic lines and the weakness of the emission of the hydrogen lines are in agreement with the hypothesis.

Consider a shell of gas in which every atomic act of line absorption is exactly compensated by a corresponding act of emission. This process is frequently defined as "scattering," because the re-emission

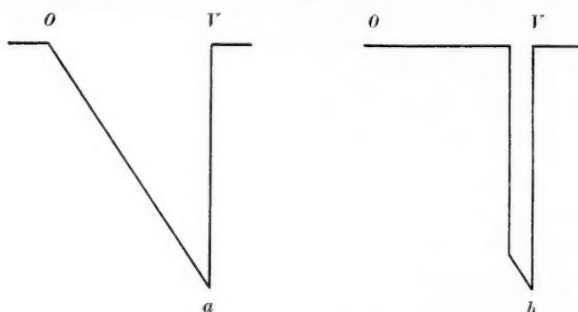


FIG. 4.—Computed contours of absorption lines formed by expanding shell of gas; (a)  $d = R$ , (b)  $d = 2R$ . Abscissa  $O$  indicates the normal wave-length of the line;  $V$  is the total velocity of expansion.

is supposed to be equally probable in all directions. The problem of the resulting line contour has been solved for two limiting cases. In the first case the radius of the star is assumed to be practically equal to the radius of the shell; this leads to the "Unsöld contour" of an absorption line. The contour is broadened if the atmosphere expands, but the effect of re-emission is merely to decrease slightly the total amount of absorbed energy. In the second case it is assumed that the diameter of the star is negligible, compared with the diameter of the shell, and it is obvious that the total emitted energy exactly compensates the total absorbed energy, provided the nebula appears as a point source on the slit of the spectrograph. Indeed, following Milne,<sup>2</sup> the light from the star, transmitted through the nebula and received by the spectrograph, is

$$L \frac{de}{4\pi\rho^2} e^{-\tau},$$

<sup>1</sup> *Ibid.*

<sup>2</sup> *Zeitschrift für Astrophysik*, 1, 109, 1930.

where  $L$  is the luminosity of the central star,  $\rho$  is the distance from the observer,  $de$  is the aperture of the telescope, and  $\tau$  is the optical thickness of the nebula. The nebular light received by the spectrograph is

$$\frac{de}{4\pi\rho^2} \pi S(1 - e^{-\tau}) 4\pi r^2,$$

where  $\pi S = L/4\pi r^2$  is the flux per cubic centimeter incident on the shell, and  $r$  is the radius of the nebula. Consequently,

$$\frac{\text{Light from star}}{\text{Light from nebula}} = \frac{e^{-\tau}}{1 - e^{-\tau}}.$$

The sum:

$$\text{Light from star} + \text{Light from nebula} = e^{-\tau} + 1 - e^{-\tau} = 1.$$

If the shell is at rest, the absorption line is exactly filled in by the emission line, and if an absorption of wave-length  $\lambda_0 + \Delta\lambda$  is followed by emission of the same  $\lambda_0 + \Delta\lambda$ , the spectrum would reveal no trace of the nebula.

If, however, the nebula is in motion, there would be a redistribution of the frequencies. This would happen, for example, if the shell is in rotation, or if it expands. In the latter case, as W. H. McCrea<sup>1</sup> has shown, the contour would resemble those observed in P Cygni stars. But in all cases the theory demands that

$$\text{Total absorption} = \text{Total emission}.$$

If neither of the two limiting assumptions is applicable, we must expect an intermediate result. The exact formulae have not been worked out, but it seems reasonable to assume that

$$\frac{\text{Total absorption}}{\text{Total emission}} = \frac{\text{Volume of shell projected upon star-disk}}{\text{Remainder of volume}}.$$

Observations of novae tend to support this assumption. In the early stages of an outburst, all lines are strongly displaced toward the violet, indicating an expanding atmosphere, but there are no emission lines. These begin to appear later, when the shell is farther re-

<sup>1</sup> *Zeitschrift für Physik*, 57, 378, 1929.

moved from the surface of the star. It should be mentioned that in novae, as well as in Wolf-Rayet stars, the equality of absorption and emission is not always obeyed. It is probable that effects of fluorescence (or recombination) upset the formulae based upon the assumption of strict compensation of absorption and emission.

In any case, it would appear to be possible to explain the weakness of the emission lines in 17 Leporis by assuming a suitable value for the ratio of  $R/d$ .

If the expanding-shell hypothesis is adopted for 17 Leporis, the occasional appearance of double lines would be interpreted as successive outbursts of gases. The faint violet component would correspond to the formation of a new shell moving outward with a high velocity. At the same time the original shell disperses into space and its lines grow rapidly weaker. The lines of the new shell are at first somewhat diffuse, but as the distance from the star increases, they become sharper. The velocity of expansion gradually decreases until a limiting velocity of 30-40 km/sec. is reached. This velocity is retained until a new outburst takes place.

While the observations definitely favor the shell rather than the binary hypothesis, we have at present no knowledge of forces that might cause the successive outbursts. Radiation pressure must probably be ruled out, because the star is not known to vary in light. Neither is it easy to explain the rapid decline in the velocities of expansion and the tendency to adopt a limiting velocity of 30-40 km/sec.

The changes in the total intensities of the lines are puzzling. Suppose that the Unsöld contour is applicable, and that in the abnormal stage half of the atoms give rise to the violet component of the line, while the other half contribute to the red. Then the total absorption in both components is

$$E_1 = 2C \sqrt{\frac{n}{2}}.$$

When the lines are single, the total emission is

$$E_2 = CVn.$$

The ratio

$$\frac{E_1}{E_2} = \frac{\sqrt[2]{n}}{\sqrt{n}} = \sqrt[2]{2}.$$

The total absorption should increase during the abnormal stage. This is true for *H*, but not for *Fe* II, *Ti* II, etc. If we assume that the weakening of the lines of *Fe* II, etc., is caused by a decrease of *n*, it would be impossible to explain the constancy of *Fe* II 4923 and the strengthening of *H*.

According to the binary hypothesis, *E* should, of course, remain constant, irrespective of whether the lines are single or double. The observed variations in *E* constitute a convincing argument against this hypothesis.

I am indebted to Dr. C. T. Elvey for the microphotometer tracings used in this paper; Messrs. W. W. Morgan, P. C. Keenan, H. F. Schwede, F. R. Sullivan, and others have participated in the observations at the telescope.

YERKES OBSERVATORY

March 19, 1932

## THE SURFACE BRIGHTNESS OF THRESHOLD IMAGES<sup>1</sup>

BY EDWIN HUBBLE

### ABSTRACT

A study of threshold images of stars photographed on Eastman 40 plates with the 100-inch and 60-inch reflectors and various cameras indicates a relation between surface brightness and size of image according to which the surface brightness diminishes as the size increases, at first rapidly and then more and more slowly. The relation has been studied for images ranging from the smallest focal images up to extra-focal images a centimeter and more in diameter. For very small images the total magnitudes are independent of the size; for very large images the surface brightness is independent of the size. The observed relation is a smooth transition between these limiting conditions.

The relation has been determined numerically for the two reflectors and used to derive statistical values for limiting magnitudes corresponding to nebular images of various dimensions.

The photographic photometry of threshold images involves an effect depending on the areas. It is well known that the photometry of surfaces differs from that of point-source images, but the manner in which the one merges into the other is seldom discussed in the literature. The question bears on the estimation of limiting magnitudes of nebulae recorded under given exposure conditions, and in this connection some data have been assembled which may be of general interest.

The investigation was limited to threshold images on Eastman 40 plates, fully developed with a hydroquinone developer (X-ray). Photographs with both the 100-inch and the 60-inch reflectors, the latter with and without the Ross zero-power correcting lens, were employed and, in addition, a few plates made with the 10-inch Cooke astrographic lens ( $f=4.5$ ) and a  $2\frac{1}{2}$ -inch Tessar ( $f=4.5$ ) were used. The plates were exposed on star fields for which the photographic magnitudes (on the international scale) were known. The star images ranged from the very small images, recorded under excellent observing conditions, through the larger images of poor seeing to extra-focal series having maximum diameters of a centimeter and more. Exposure times ranged from one minute to

<sup>1</sup> *Contributions from the Mount Wilson Observatory, Carnegie Institution of Washington*, No. 453.



an hour or more, but the results were reduced to a standard exposure of one minute, on the usual assumption that tripling the exposure increases the limit of the plate by 1 mag. Analysis of the data indicates that for the present purpose errors arising from this assumption are negligible.

The observations consisted in (1) measuring the diameters of the faint images and (2) estimating the limiting magnitude of the plate by identifying the faintest stars that could be detected, either with or without optical aid. The surface brightness corresponding to the threshold image was then derived by spreading the luminosity equivalent to the limiting magnitude over the area of the image.

Let  $d$  be the diameter of the image in seconds of arc,  $A$  its area, and  $m$  the limiting magnitude of the plate. The surface brightness producing the threshold image in magnitudes per unit area of 1 square second, is then<sup>1</sup>

$$\begin{aligned} SB &= m + 2.5 \log A, \\ &= m - 0.26 + 5 \log d = m + \Delta A. \end{aligned}$$

In the case of extra-focal images obtained with the reflectors, it is necessary to correct the area for the shadow of the Newtonian flat and its supports.

The surface brightness producing a threshold image is measured by the quantity of light reaching the plate divided by the area of the image. When threshold images of the same linear dimensions are produced with different telescopes, then, for the quantity of light to remain constant, the luminosity of the light-source, i.e., the star whose image is recorded, must vary inversely with the square of the aperture. The necessary correction might be applied directly in the calculation of surface brightness, but for telescopes of the same focal ratio it is conveniently introduced by expressing the area of the image in angular units. Since the angular area also varies inversely as the square of the aperture (or focal length), the effect of the aper-

<sup>1</sup> The expression is derived as follows:

$$\text{Surface brightness} = \frac{\text{Luminosity}}{\text{Area}},$$

$$\log SB = \log L - \log A.$$

Since  $m$  (magnitude) = Const.  $- 2.5 \log L$ ,  $SB$  (in  $m$  per unit area) =  $m + 2.5 \log A$ .

ture is canceled. Hence, when the surface brightness is thus expressed in magnitudes per unit area of 1 square second of arc on the scale of the telescope in question, the results for all telescopes of a given focal ratio are numerically on a single homogeneous scale and are directly comparable.

In the present discussion the bulk of the data is derived from plates with the 100-inch and 60-inch reflectors and the scale represents a Newtonian reflector with a focal ratio of  $f=5$ . Results for other types of telescopes, in order to conform to the same scale, must be corrected by the amount

$$\Delta SB = 5 \log \frac{F'}{F},$$

where  $F'$  and  $F$  are the focal ratios of the telescope in question and of the standard type, respectively.

The data are listed in Table I. Exposures are given in minutes and diameters in seconds of arc;  $\Delta A$ ,  $\Delta E$ , and  $\Delta Z$  are corrections for area, exposure time, and zenith distance, by which the observed limiting magnitudes,  $m$ , are reduced to surface brightness,  $SB$ , in magnitudes per square second of arc for a standard exposure of one minute. The last column lists  $\log D$ , where  $D$  is the diameter expressed in millimeters.  $SB$  and  $\log D$  are the significant quantities, and Figure 1 exhibits the correlation between them. The points for the various telescopes are mingled in the one diagram, but are represented by different symbols. Diameters range from 0.025 to 13.4 mm, and the surface brightness from about 16 to 21 mag. per square second. Over the entire range there is a close correlation between the two quantities.

The three sets of data for the two reflectors may be discussed as a homogeneous group. The individual curves are roughly parallel, and the relatively slight displacements may be disregarded in a first approximation. The mean correlation-curve indicates that the surface brightness producing threshold images diminishes as the diameters increase, at first rapidly, then more and more slowly. The curve appears to depart asymptotically from a straight line  $A$  and approach asymptotically a horizontal line  $B$ , whose level is not determined by the present data.

TABLE Ia

100-INCH REFLECTOR; SCALE, 1 MM=16".0

| Plate                   | Field   | Exp. | <i>d</i> | <i>m</i> | $\Delta A$ | $\Delta E$ | $\Delta Z$ | <i>SB</i> | log <i>D</i> |
|-------------------------|---------|------|----------|----------|------------|------------|------------|-----------|--------------|
|                         |         | Min. |          |          |            |            |            |           |              |
| H 68.....               | S.A. 87 | 2    | 0.8      | 17.75    | -0.75      | -0.63      | +0.02      | 16.39     | -1.30        |
| 69.....                 | 87      | 2    | 0.9      | 17.8     | 0.49       | 0.63       | .02        | 16.70     | 1.25         |
| 487.....                | 45      | 3    | 0.9      | 17.8     | 0.49       | 1.0        | .02        | 16.33     | 1.25         |
| SS 5505.....            | 87      | 2    | 1.1      | 17.67    | 0.06       | 0.63       | .03        | 17.01     | 1.16         |
| 5507.....               | 87      | 2    | 1.1      | 17.65    | -0.06      | 0.63       | .03        | 16.99     | 1.16         |
| 5506.....               | 87      | 2    | 1.2      | 17.64    | +0.13      | 0.63       | .03        | 17.17     | 1.12         |
| H <sub>i</sub> 930..... | 61      | 3    | 1.2      | 18.3     | 0.13       | 1.0        | .00        | 17.43     | 1.12         |
| H 683.....              | 44      | 15   | 1.3      | 19.4     | 0.31       | 2.47       | .02        | 17.26     | 1.09         |
| 618.....                | 45      | 6    | 1.3      | 18.1     | 0.27       | 1.63       | .01        | 16.75     | 1.09         |
| D 424.....              | 65      | 3    | 1.4      | 18.45    | 0.47       | 1.0        | .00        | 17.92     | 1.06         |
| H 613.....              | 45      | 3    | 1.4      | 17.4     | 0.47       | 1.0        | .05        | 16.92     | 1.06         |
| H <sub>i</sub> 4.....   | 87      | 5    | 1.6      | 18.36    | 0.76       | 1.47       | .03        | 17.68     | 1.00         |
| 5.....                  | 87      | 3    | 1.6      | 17.84    | 0.76       | 1.0        | .03        | 17.63     | 1.00         |
| H 684.....              | 44      | 10   | 1.6      | 18.6     | 0.76       | 2.10       | .07        | 17.33     | 1.00         |
| H <sub>i</sub> 6.....   | 87      | 3    | 1.7      | 17.83    | 0.89       | 1.0        | .03        | 17.75     | 0.97         |
| H 863.....              | 45      | 15   | 1.7      | 19.3     | 0.89       | 2.47       | .02        | 17.74     | 0.97         |
| 319.....                | 136     | 10   | 2.0      | 18.2     | 1.24       | 2.10       | .18        | 17.52     | 0.90         |
| H <sub>i</sub> 10.....  | 45      | 30   | 2.0      | 19.1     | 1.24       | 3.10       | .02        | 17.26     | 0.90         |
| H 1178.....             | 45      | 1    | 2.3      | 16.15    | 1.55       | 0.0        | .07        | 17.77     | 0.84         |
| 1136.....               | 45      | 3    | 2.4      | 17.5     | 1.64       | 1.0        | .00        | 18.14     | 0.82         |
| 1210.....               | 51      | 5    | 2.8      | 17.6     | 1.97       | 1.47       | .00        | 18.10     | 0.76         |
| 1220.....               | 51      | 5    | 2.8      | 17.6     | 1.97       | 1.47       | .00        | 18.10     | 0.76         |
| 1221.....               | 77      | 8    | 3.3      | 18.2     | 2.33       | 1.89       | .03        | 18.69     | 0.69         |
| 1009.....               | 45      | 3    | 3.4      | 16.9     | 2.40       | 1.0        | .00        | 18.30     | 0.67         |
| 1008.....               | 45      | 60   | 4.6      | 19.3     | 3.05       | 3.73       | .02        | 18.62     | 0.54         |
| 1222.....               | *       | 60   | 10.0     | 18.45    | +4.74      | -3.73      | +0.02      | 19.48     | -0.20        |
| Extra-Focal             |         |      |          |          |            |            |            |           |              |
| H <sub>i</sub> 930..... | 61      | 3    | 6.4      | 16.8     | +3.50      | -1.0       | 0.00       | 19.30     | +0.40        |
| D 426.....              | 65      | 1    | 6.5      | 15.85    | 3.60       | 0.0        | + .02      | 19.47     | .39          |
| 424.....                | 65      | 3    | 6.8      | 16.6     | 3.66       | 1.0        | .00        | 19.26     | .37          |
| H <sub>i</sub> 930..... | 61      | 3    | 12.4     | 15.9     | 5.0        | 1.0        | .00        | 19.90     | .11          |
| H 761.....              | *       | 30   | 14.4     | 17.45    | 5.35       | 3.1        | .00        | 19.70     | .05          |
| 1171.....               | 45      | 1    | 14.4     | 14.3     | 5.4        | 0.0        | .00        | 19.70     | + .05        |
| D 424.....              | 65      | 3    | 14.8     | 15.45    | 5.45       | 1.0        | .00        | 19.90     | - .03        |
| H <sub>i</sub> 930..... | 61      | 3    | 30.0     | 14.2     | 7.0        | 1.0        | .00        | 20.20     | + .27        |
| D 424.....              | 65      | 3    | 30.4     | 14.2     | 7.03       | 1.0        | .00        | 20.23     | .28          |
| H 1171.....             | 45      | 1    | 31.6     | 13.4     | 7.11       | 0.0        | .00        | 20.51     | .30          |
| 1178.....               | 45      | 3    | 40.0     | 13.7     | 7.63       | 1.0        | + .07      | 20.40     | .40          |
| 1136.....               | 45      | 3    | 56.0     | 13.45    | +8.36      | -1.0       | 0.00       | 20.81     | +0.54        |

\* Fields in which magnitudes are known from comparisons with Selected Areas.

TABLE Ib

60-INCH REFLECTOR; SCALE, 1 MM = 27".2

| Plate                 | Field   | Exp | <i>d</i> | <i>m</i> | $\Delta A$ | $\Delta E$ | $\Delta Z$ | <i>SB</i> | log <i>D</i> |
|-----------------------|---------|-----|----------|----------|------------|------------|------------|-----------|--------------|
| Min.                  |         |     |          |          |            |            |            |           |              |
| S 838.....            | S.A. 17 | 2   | 1".0     | 17.45    | -0.26      | -0.63      | +0.04      | 16.60     | -1.44        |
| 840.....              | 42      | 1   | 1.1      | 16.7     | 0.06       | 0.0        | .01        | 16.65     | 1.40         |
| S <sub>1</sub> 1..... | 87      | 5   | 1.1      | 17.82    | 0.06       | 1.47       | .03        | 16.32     | 1.40         |
| 2.....                | 87      | 3   | 1.1      | 17.61    | 0.06       | 1.0        | .03        | 16.59     | 1.40         |
| 3.....                | 87      | 2   | 1.1      | 16.85    | -0.06      | 0.63       | .03        | 16.10     | 1.40         |
| S 835.....            | 16      | 2   | 1.2      | 17.3     | +0.13      | 0.63       | .04        | 16.84     | 1.36         |
| 830.....              | 17      | 5   | 1.4      | 18.1     | 0.47       | 1.47       | .05        | 17.15     | 1.20         |
|                       | 17      | 2   | 1.4      | 17.3     | 0.47       | 0.63       | .05        | 17.19     | 1.20         |
| 839.....              | 42      | 5   | 1.4      | 18.0     | 0.47       | 1.47       | .02        | 17.02     | 1.20         |
| 992.....              | 62      | 3   | 1.6      | 17.3     | 0.76       | 1.0        | .02        | 17.08     | 1.23         |
|                       |         | 1   | 1.6      | 16.2     | 0.76       | 0.0        | .02        | 16.98     | 1.23         |
|                       | 62      | 3   | 1.8      | 17.5     | 1.01       | 1.0        | .02        | 17.53     | 1.18         |
| 993.....              |         | 1   | 1.8      | 16.3     | 1.01       | 0.0        | .02        | 17.33     | 1.18         |
| 890.....              | 23      | 1   | 2.0      | 16.5     | 1.24       | 0.0        | .01        | 17.75     | 1.14         |
| 878.....              |         | 3   | 2.5      | 17.2     | 1.73       | 1.0        | .04        | 17.97     | 1.04         |
|                       | 45      | 1   | 2.5      | 16.2     | 1.73       | 0.0        | .04        | 17.97     | 1.04         |
| 877.....              |         | 3   | 2.7      | 17.2     | 1.89       | 1.0        | .04        | 18.13     | 1.01         |
|                       | 45      | 1   | 2.7      | 16.0     | 1.89       | 0.0        | .04        | 17.93     | 1.01         |
| 881.....              |         | 3   | 2.7      | 17.2     | 1.89       | 1.0        | .07        | 18.16     | 1.01         |
|                       | 92      | 1   | 2.7      | 16.3     | 1.89       | 0.0        | .07        | 18.26     | 1.01         |
| 920.....              | 105     | 20  | 8.0      | 17.7     | +4.25      | -2.73      | +0.07      | 19.29     | -0.53        |
| Extra-Focal           |         |     |          |          |            |            |            |           |              |
| 562.....              | *       | 60  | 10.0     | 18.4     | +4.60      | -3.73      | +0.03      | 19.30     | -0.44        |
| 727.....              | *       | 50  | 12.0     | 18.2     | 5.00       | 3.57       | .13        | 19.76     | .36          |
| 519.....              | *       | 30  | 18.0     | 17.1     | 5.88       | 3.10       | .01        | 19.89     | -.18         |
| 908.....              | *       | 60  | 32.0     | 17.0     | 7.14       | 3.73       | .03        | 20.44     | +.07         |
| 832.....              | *       | 50  | 34.4     | 17.0     | 7.29       | 3.57       | .00        | 20.72     | .10          |
| 820.....              | *       | 60  | 35.6     | 17.0     | 7.37       | 3.73       | .02        | 20.66     | .11          |
| 828.....              | *       | 60  | 38.4     | 16.35    | 7.54       | 3.73       | .05        | 20.21     | .15          |
| 852.....              | *       | 60  | 43.8     | 16.5     | 7.83       | 3.73       | .04        | 20.64     | .20          |
| 848.....              | *       | 60  | 50.7     | 16.2     | 8.13       | 3.73       | .10        | 20.70     | .27          |
| 865.....              |         | 94  | 52.0     | 13.6     | 8.20       | 1.0        | .07        | 20.87     | .28          |
| 919.....              | 13      | 3   | 53.5     | 13.4     | 8.26       | 1.0        | .03        | 20.69     | .29          |
| 864.....              | 94      | 15  | 55.0     | 14.9     | 8.32       | 2.47       | .07        | 20.82     | .30          |
| 883.....              | *       | 60  | 55.0     | 15.7     | 8.32       | 3.73       | .24        | 20.54     | .30          |
| 800.....              | 23      | 3   | 56.0     | 13.6     | 8.36       | 1.0        | .01        | 20.97     | .31          |
| 841.....              | *       | 40  | 61.1     | 15.8     | 8.55       | 3.36       | .06        | 21.05     | .35          |
| 842.....              | *       | 60  | 63.0     | 15.6     | 8.61       | 3.73       | .04        | 20.52     | .36          |
| 882.....              | 92      | 3   | 74.0     | 13.4     | 8.96       | 1.0        | .07        | 21.43     | .43          |
| 880.....              | *       | 60  | 75.0     | 15.5     | +8.99      | -3.73      | +0.01      | 20.77     | +0.44        |

\* Fields in which magnitudes are known from comparisons with Selected Areas.

## BRIGHTNESS OF THRESHOLD IMAGES

III

TABLE Ic

ROSS CORRECTOR ON 60-INCH REFLECTOR; SCALE, 1 MM = 26".6

| Plate       | Field   | Exp. | <i>d</i> | <i>m</i> | $\Delta A$ | $\Delta E$ | $\Delta Z$ | <i>SB</i> | log <i>D</i> |
|-------------|---------|------|----------|----------|------------|------------|------------|-----------|--------------|
|             |         | Min. |          |          |            |            |            |           |              |
| S 1055*     | S.A. 45 | 1    | 2".26    | 16.25    | + 1.51     | 0.00       | +0.19      | 17.95     | -1.07        |
| 1054*       | 45      | 1    | 2.39     | 16.4     | 1.63       | .00        | .18        | 18.21     | 1.05         |
| 1049*       | 45      | 1    | 2.53     | 16.15    | 1.75       | .00        | .00        | 17.90     | 1.02         |
| 1052*       | 45      | 1    | 2.79     | 16.25    | 1.96       | .00        | .02        | 18.23     | 0.98         |
| P 1*        | Pole    | 1    | 2.79     | 16.0     | 1.96       | .00        | .24        | 18.20     | 0.98         |
| S 1050*     | 45      | 1    | 2.93     | 16.65    | 2.07       | .00        | .00        | 18.72     | 0.96         |
| P 2*        | Pole    | 1    | 2.93     | 14.85    | + 2.07     | 0.00       | +0.24      | 17.16     | -0.96        |
| Extra-Focal |         |      |          |          |            |            |            |           |              |
| S 980.....  | Pole    | 40   | 75.8     | 15.1     | + 9.10     | -3.36      | +0.24      | 21.08     | +0.45        |
| 1033.....   | †       | 80   | 179.0    | 14.5     | 10.81      | 3.99       | .03        | 21.35     | 0.83         |
| 1046.....   | Pole    | 80   | 187.0    | 14.0     | 10.99      | 3.99       | .24        | 21.24     | 0.85         |
| 1027.....   | †       | 90   | 212.0    | 14.2     | 11.22      | 4.10       | .09        | 21.41     | 0.90         |
| 1005.....   | †       | 65   | 214.0    | 13.5     | 11.22      | 3.80       | .09        | 21.01     | 0.90         |
| 1022.....   | †       | 70   | 220.0    | 14.0     | 11.26      | 3.87       | .18        | 21.57     | 0.92         |
| 1024.....   | †       | 60   | 287.0    | 12.8     | 11.85      | 3.73       | .08        | 21.00     | 1.03         |
| 1032.....   | †       | 80   | 343.0    | 13.0     | 12.25      | 3.99       | .09        | 21.35     | 1.11         |
| 1023.....   | †       | 65   | 350.0    | 12.5     | +12.34     | -3.80      | +0.10      | 21.14     | +1.13        |

\* Values of *m* and *d* are means of two or three exposures on a single plate.

† Fields in which magnitudes are known from comparisons with Selected Areas.

TABLE Id

| Plate                                  | Field   | Exp. | <i>d</i> | <i>m</i> | $\Delta A$ | $\Delta E$ | $\Delta Z$ | <i>SB</i> * | log <i>D</i> |
|--|---------|------|----------|----------|------------|------------|------------|-------------|--------------|
| 10-Inch Cooke Lens; Scale, 1 mm = 180" |         |      |          |          |            |            |            |             |              |
|  |         | Min. |          |          |            |            |            |             |              |
| †.....                                 | Pole    | 1    | 3.6      | 12.6     | + 2.52     | 0.00       | +0.24      | 15.36       | -1.70        |
| †.....                                 | Pole    | 10   | 5.0      | 14.8     | 3.33       | -2.10      | .24        | 16.27       | 1.57         |
| †.....                                 | Pole    | 8    | 12.6     | 14.9     | 5.24       | 1.80       | .24        | 18.49       | 1.15         |
| T 143.....                             | †       | 60   | 90.0     | 14.3     | 9.51       | 3.73       | .04        | 20.12       | 0.30         |
| T 120.....                             | †       | 60   | 126.0    | 13.7     | +10.24     | -3.73      | +0.04      | 20.25       | -0.15        |
| 2½-Inch Tessar; Scale, 1 mm = 830"     |         |      |          |          |            |            |            |             |              |
| t 21.....                              | S.A. 80 | 120  | 16.0     | 14.1     | + 5.85     | -4.36      | +0.02      | 15.61       | -1.70        |
| t 33.....                              | 64      | 105  | 20.0     | 14.7     | 6.32       | 4.24       | .00        | 16.78       | 1.60         |
| t 10.....                              | 80      | 60   | 360.0    | 12.3     | +12.60     | -3.73      | +0.03      | 21.20       | -0.35        |

\* Since the 10-inch and the 2½-inch cameras have a focal ratio of  $f=4.5$ , corrections of  $-0.23$  are required to reduce the values of *SB* to the system of the reflectors.† Values of *m* and *d* are means from three plates.

‡ Fields in which magnitudes are known from comparisons with Selected Areas.

The line *B* represents what would be found were the surface brightness required to produce a threshold image independent of the size of the image and constant for a given exposure. This line is approached as the images become very large.

The slope of *A*, on the other hand, is such that the line corresponds to the case in which the total luminosity, and not the surface brightness, is independent of the size of the image; in other words, data

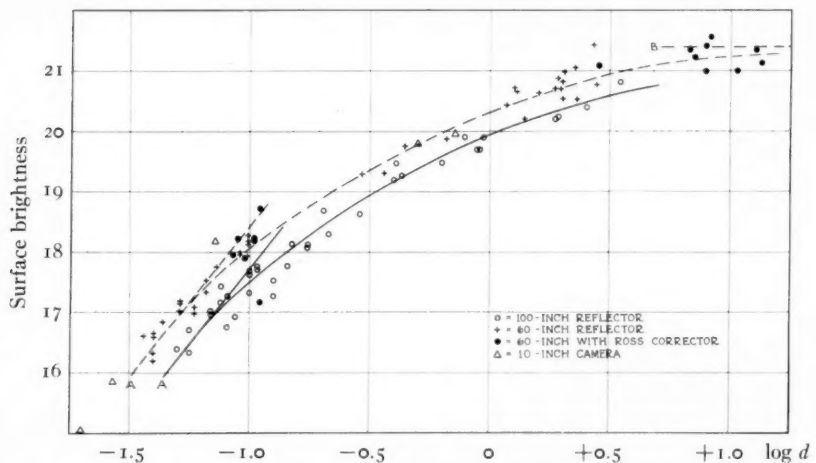


FIG. 1.—Relation between surface brightness and diameter of threshold images. The data are derived from threshold images of stars on Eastman 40 plates and are reduced to uniform exposures of one minute. Diameters are expressed in millimeters and surface brightness in photographic magnitudes per square second of arc.

represented by *A* would indicate that the limiting magnitudes of plates having the same exposures are independent of the size of the threshold images. The observations show that the relation holds very closely for small images.

This result explains several otherwise curious points in the behavior of images. For instance, with the 100-inch reflector, diameters of star images vary from 1".0 to 2".0 as the seeing varies from "good" to "fair." The areas of the images thus vary from 1 to 4, and one might expect the limiting magnitude for a given exposure to range through 1.5 mag. Actually, the range is only about 0.5 mag., a value which is consistent with the present correlation. The change



in surface brightness producing the threshold images is nearly compensated by the change in area.

The correlation-curve appears to represent a smooth transition between the two limiting cases indicated by lines *A* and *B*. The analogy with the threshold sensitivity of the retina for faint light-sources is close. For small sources, the determining factor in producing a visual sensation is the total luminosity, and not the surface brightness; for very large sources, it is the surface brightness alone. The transition between the two cases is roughly similar to that exhibited in Figure 1.

The photographic data suggest that the eye may react to dark images on a luminous background in much the same fashion as to luminous images on a dark background; in other words, that the correlation of Figure 1, in part at least, expresses a physiological phenomenon. But photographic phenomena are probably also involved in addition to the laws of visual perception. This conclusion seems to follow from the fact that small images were studied with magnifications up to  $\times 12$ , while large images were examined with the unaided eye. In consequence, the angular diameters of magnified images frequently exceeded those of larger images examined with less magnification or with none at all. Moreover, the small threshold images are detected as loose patterns of isolated silver grains and offer problems quite distinct from those involved in the visual perception of continuous surfaces. We may, however, refrain from assigning the parts played by the eye and by the plate, and merely state that the visual examination of threshold images on photographic negatives conforms to the same general pattern as the visual examination of faint luminous sources against a dark background.

The results for the various instruments are very similar. The small systematic displacements of the individual curves indicate a slight increase in the efficiency as the size of instrument decreases. The surface brightness corresponding to images one-sixteenth of a millimeter in diameter ( $1''.0$  on the scale of the 100-inch) is as shown in the accompanying tabulation. A few plates with a  $2\frac{1}{4}$ -inch Tessar,  $f=4.5$ , suggest a value of the order of 17.7 for this small camera, and

two plates taken at the Cassegrain focus of the 60-inch<sup>1</sup> indicate a value about 15.8.

| Instrument          | Focal Length | <i>SB</i> |
|---------------------|--------------|-----------|
| 100-inch.....       | 505          | 16.75     |
| 60-inch.....        | 300          | 17.35     |
| 60-inch (Ross)..... | 306          | (17.4)*   |
| 10-inch.....        | 45           | 17.55     |

\* Extrapolation.

The scattering of the points for a single instrument represents errors arising from many sources. The probable error in the estimation of limiting magnitudes is believed to be of the order of 0.1 mag. The percentage errors in measuring diameters are negligible for large images but become increasingly important as diameters decrease. For instance, an error of 0.005 mm in images 0.04 mm in diameter represents an error in the surface brightness of the order of 0.3 mag. Differences in plate sensitivity, development, sky transparency, and reflectivity of mirrors are also included in the scattering. The average deviation, however, appears to be less than 0.2 mag., from which may be inferred the order of the probable errors in statistical investigations that involve limiting magnitudes on uncalibrated exposures.

Among the various applications of the correlation diagram is the estimation of limiting magnitudes of nebulae which can be recognized as such on exposures of various lengths. The last recognizable traces of nebulae appear as small spots of approximately uniform density, distinguished from stars merely by their larger areas. The minimum diameters are of the order of two to three times the diameters of faint star images, varying, of course, with the personal equation of the observer. From this it follows that, with large reflectors, the limiting magnitudes for nebulae range from 0.5 to 1.0 mag. brighter than those for stars.

For example, on excellent plates with the 100-inch, the minimum diameters of recognizable nebulae are between 3" and 4". For exposures of an hour, threshold images of this size represent total

<sup>1</sup> The actual measures are 15.1 mag. per square second for images with diameters of 0.25 mm, or 2".2. The correction due to the focal ratio,  $f=16.0$ , is about +2.6 mag. The point falls below the curve in Fig. 1 by about 1.5 mag.

photographic magnitudes of from 19.9 to 19.6. The value adopted by the writer is 19.8, probably a full magnitude brighter than the limiting magnitude for stars. Corrections are necessary for less favorable observing conditions and, of course, the interpretation of the data is complicated by the difficult question as to what fraction of the total luminosities of nebulae is represented by the threshold images.

The correlation has not been investigated for densities above the threshold of the plates. It is presumed that the effect diminishes as the density increases and eventually becomes negligible. The magnitude is so considerable at the threshold, however, that the effect is probably appreciable among faint images in general.

The displacement between the correlation-curves for the 60-inch and 100-inch reflectors is unexpected. The two curves appear to be roughly parallel throughout the observed range, the displacement amounting to about 0.5 mag. for the small images and 0.35–0.4 mag. for large ones. The reality of the displacement for small images is confirmed by an inspection of the limiting magnitudes of the focal images. The limiting magnitudes for exposures of one minute vary systematically with the diameters, but are fairly constant for the smallest images at mean values of 17.2 and 16.6 for the 100-inch and 60-inch, respectively. The difference, 0.6 mag., differs from the theoretical value derived from the ratio of apertures, namely, 1.11 mag., by 0.5 mag.—nearly the amount of the displacement in this region of the correlation-curve. When the diameters are expressed in seconds of arc instead of in millimeters, the displacement is almost negligible.

The explanation of the displacement has not yet been determined. Systematic differences in the mirrors seem improbable since the observations range over several years. It is possible that the curves actually converge for the large images and that the displacement arises from accidental scatter of the limited number of points observed. This argument does not apply with equal force to the smaller images, where, moreover, the displacement is emphasized by the data for the smaller instruments.

The danger of overinterpretation is emphasized by the data for the 60-inch reflector obtained with the Ross correcting lens. These represent careful and very consistent observations made by Mr. N. U.

Mayall at the writer's request. Each observer establishes arbitrary standards in the difficult task of examining threshold images, and hence minor differences are to be expected, although the general run of the correlation-curves should be similar. Mayall's data for small images lie slightly above the writer's results for the 60-inch without the correcting lens, although the lens loses about 0.2 mag. by reflection and absorption. For the larger images, the two sets of data tend to merge. This is consistent with the suggestion that the curves for the 60-inch and 100-inch instruments also tend to merge as the areas increase and that the observed displacement in those regions may represent accidental scattering.

The faintest surface brightness actually observed is represented by the mean value for five plates taken with the Ross correcting lens on the 60-inch reflector with exposures ranging from seventy to ninety minutes. The data are:

$$\begin{aligned}\log E &= 1.902 \text{ (} E = 80 \text{ min.) ,} \\ \log D &= 0.921 \text{ (} D \text{ in millimeters) ,} \\ SB &= 25.24 \text{ mag. per square second.}\end{aligned}$$

Since the correlation-curve is still rising in this region and since the small cameras appear to be more efficient than the large reflectors, it is probable that the cameras would register 26 mag. per square second in two hours for images with areas of a few square centimeters. A reasonable limit for prolonged exposures under the best conditions is probably between 26.5 and 27 mag.—say 9 mag. per square degree. This refers to cameras with speeds of the order of  $f=4.5$  or  $f=5$ . It is doubtful, in view of the general luminosity of the sky, whether faster cameras would offer greater advantage except in the matter of reducing the exposure time.

CARNEGIE INSTITUTION OF WASHINGTON  
MOUNT WILSON OBSERVATORY  
March 1932

## AN APPLICATION OF THE RADIOMETER: A REGISTERING MICROPHOTOMETER<sup>1</sup>

By SINCLAIR SMITH and OLIN C. WILSON, JR.

### ABSTRACT

A registering microphotometer is described in which a radiometer is used as the light-sensitive element. The instrument has been made as simple as possible without sacrifice of performance, and tests seem to show that it is both fast and precise, besides being very easy to operate. The details of construction are discussed and some typical records are reproduced.

Thus far, registering microphotometers have been of two kinds, those using a photoelectric cell for the light-sensitive element, and those making use of the thermocouple. A radiometer can also be used as the light-sensitive element, and it offers some advantages over each of the other two devices. For the same period of oscillation it is inherently more sensitive than a thermocouple and galvanometer and is of course not subject to the various electrical difficulties accompanying the use of a photocell and electrometer. For laboratories that prefer to build their own instruments it has the further advantage of being relatively simple to construct, while the other devices usually require the services of specialists.

A registering microphotometer having a radiometer as the light-sensitive element has been built at the Mount Wilson Observatory and is now in regular service. The main feature of this instrument, aside from the radiometer, is the elimination of the usual gear or lever system between the plate carriage and the recording film-holder. Instead, electric-clock motors drive the two parts separately. Since the advent of electric clocks, small synchronous motors having built-in reduction-gears can be obtained at a very small cost.

As originally assembled, the microphotometer here described was an attachment to a comparator. A slit was substituted for the eyepiece of the comparator microscope, and a second microscope objective was mounted on the comparator base. The plate to be studied was mounted in its usual position. The slit image was focused on

<sup>1</sup> *Contributions from the Mount Wilson Observatory, Carnegie Institution of Washington*, No. 454.

the plate, and the light which passed through the emulsion was collected by the second microscope objective and focused on one of the vanes of a radiometer. The plate was driven by a Telechron clock motor geared to the screw of the comparator, while a second clock motor drove the recording film upon which was registered the deflection of the radiometer.

As the performance of the instrument was excellent as regards both speed and accuracy, a special plate carriage was constructed and the whole assembly made permanent. The general arrangement is shown in Plate XII *a*. The details of construction follow.

#### THE RADIOMETER

In order to serve as the light-sensitive element of a microphotometer, a radiometer should fulfil the following requirements. Besides sensitivity, if the microphotometer is to be reasonably fast, the radiometer must have a short period. It should be critically damped with good approximation and must carry a mirror of sufficient size to give a narrow line on the recording film. These conditions are satisfied by the radiometer shown in Figure 1.



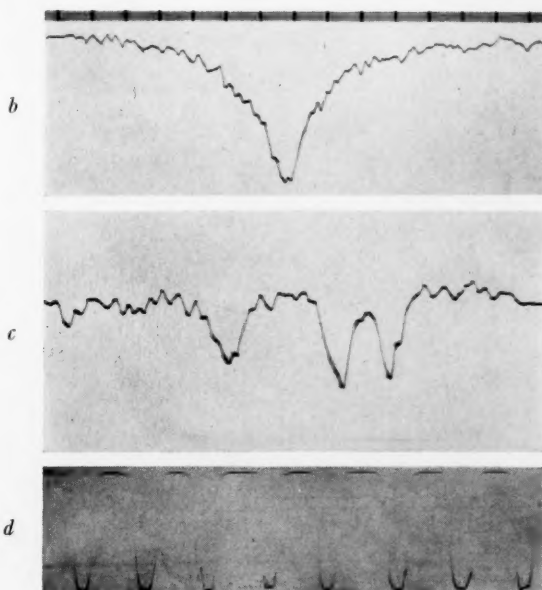
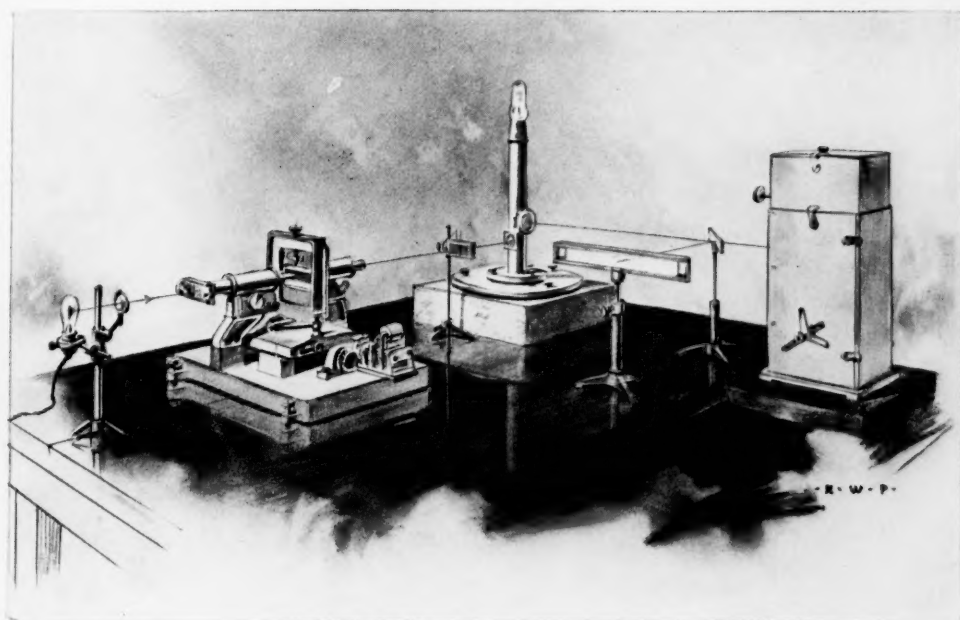
FIG. 1.—The radiometer.

A central staff of glass 0.1 mm in diameter supports the mirror and two cross-arms, also of glass, about 0.04 mm in diameter. The cross-arms carry the vanes, each of which is double, as shown in the figure. The various parts are joined together with minute particles of shellac, fused by the radiation from a small electrically heated wire.

The vanes, which are  $1 \times 3$  mm, are made of mica somewhat under  $1 \mu$  in thickness. Small sheets of the proper thickness can be cleaved from poor-quality mica (good-quality mica must be carefully avoided) with the aid of a sharp scalpel, the right thickness being recognizable by the fact that light reflected by the mica appears either red or green. The vanes are blackened on the side to be exposed to radiation. For this purpose carbon-black or lampblack, suspended in alcohol to which has been added one drop of turpentine to each

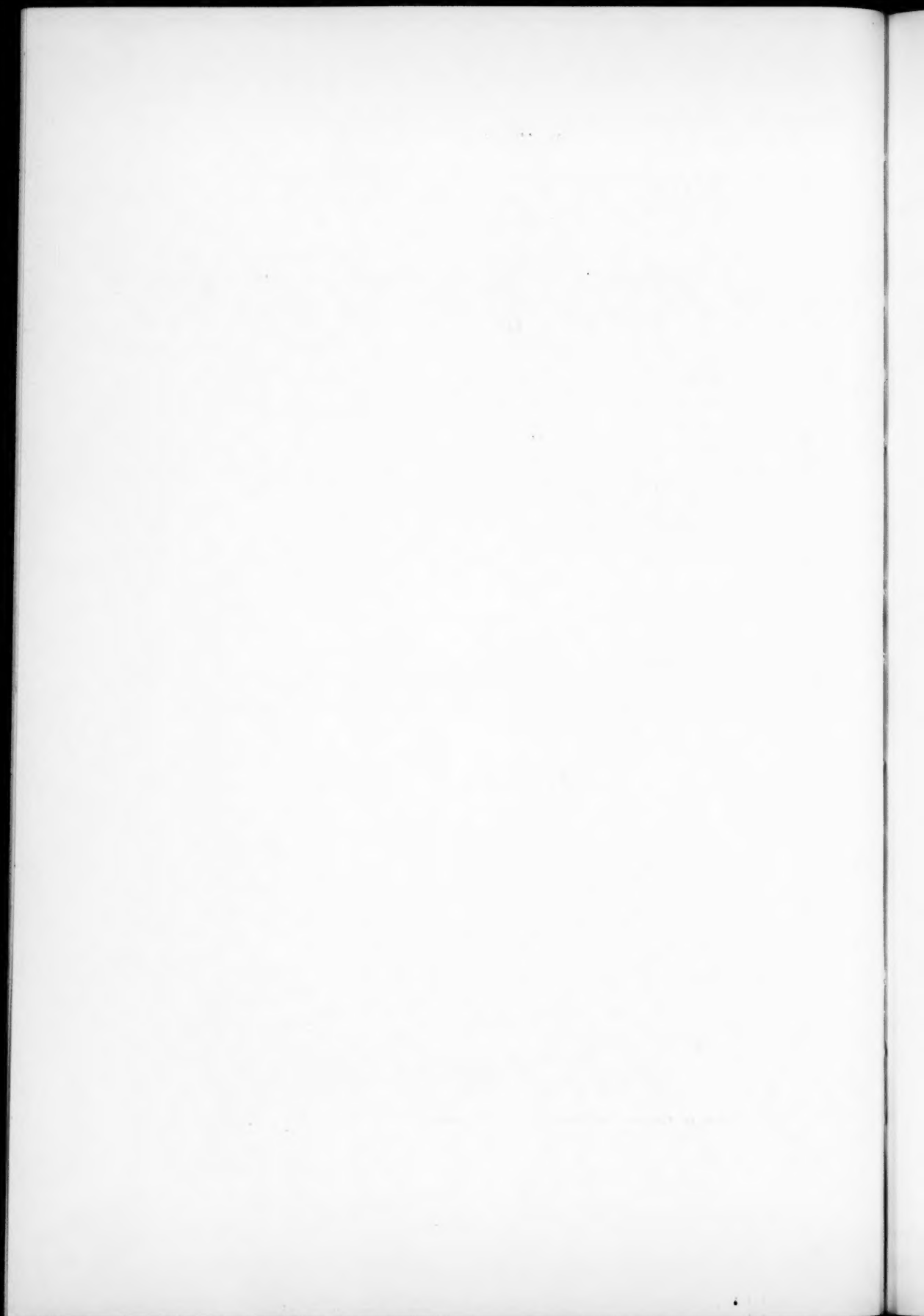


# PLATE XII



*a*, General view of the microphotometer; *b*, *c*, *d*, some typical microphotometer tracings





3 cc of alcohol, makes a good "paint." It should be put on in a very thin layer with a small sable brush.

The radiometer mirror, approximately  $2.5 \times 2.5$  mm, is cleaved from a sheet of calcite that has been polished on one side and then fine-ground down to a thickness of about 0.05 mm. Calcite yields thin mirrors having a better optical figure than those made from glass or quartz. The mirror is sputtered with either silver or platinum and afterward attached to the radiometer staff with a minute speck of shellac. In case the mirror proves to be astigmatic, it should be mounted with one of the axes of astigmatism parallel to the staff.

The radiometer is suspended on a quartz fiber 20 cm long and of sufficient cross-section to give a period of oscillation of approximately 0.2 sec.

The radiometer chamber consists of a short length of heavy-wall copper tubing, one end of which is soldered to a brass base-plate and the other tapered to fit the outer portion of a standard glass ground-joint from which the removable cap is made. A loose-fitting plug, resting on a shoulder inside the main tube, carries a short adjustable rod to which the upper end of the quartz fiber is attached. Short lengths of tubing soldered to the main tube carry the necessary windows both for the incoming radiation and for the recording light.

A stopcock sealed to the chamber enables one to evacuate the chamber and introduce the proper gas. For routine work the radiometer has been used with helium at a pressure of 1 mm. At lower pressures the radiometer is more sensitive, but the instrument becomes seriously underdamped.

#### THE PLATE CARRIAGE

The plate carriage is shown in Figure 2. The carriage rides above the base casting on four steel balls in V-grooves. The base casting also carries the driving motor, a reversible Telechron, and the screw, which is mounted in ball-bearings. Two adjustable cone-bearings at one end of the screw can be set for no end play, while a self-centering bearing serves at the other end. Two driving speeds are provided for by two gears on the driving motor, either of which can be meshed with a gear on the screw. The actual plate speed used must of course depend on the type of detail one wishes to study.

The photographic plate to be studied is mounted on a vertical cross-slide on the upper part of the carriage. As shown in Figure 2, this part of the carriage is pivoted on the lower part and can be tilted by means of a tangent screw. This enables one to line up a plate accurately with the direction of motion. Lining-up is also facilitated by the fact that the carriage can be released from the screw and moved freely by simply depressing a lever on the carriage. Two parallel jaws, one of which is movable, are mounted on the lower part of the carriage and grip a steel ball mounted on the upper part of the nut. There is no other constraint on the nut. A slight motion

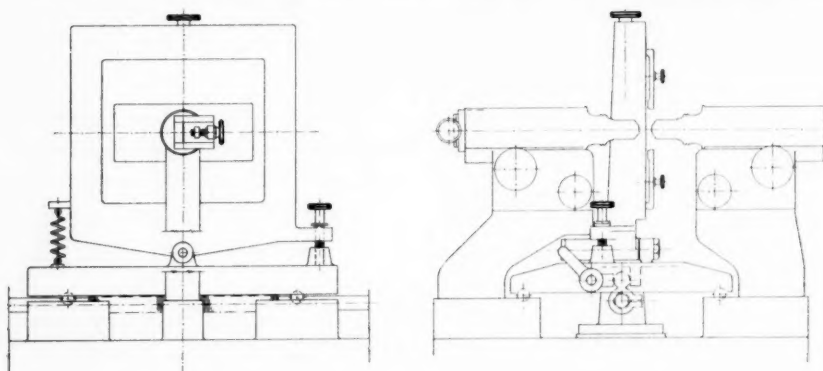


FIG. 2.—The plate carriage

of the movable jaw by means of the lever enables one to clamp or release the carriage at any point on its run.

Brackets on the base carry the two microscope tubes and focusing racks. Both tubes are fitted with 16-mm objectives; one tube carries the slit, the other is open.

#### THE RECORDING FILM CAMERA

Records are made on double-width (i.e., 70-mm) moving-picture film. The camera, shown in Figure 3, consists of two parts. The lower part, containing a supply of unexposed film, the driving mechanism, etc., remains in a fixed position, while the upper part, which receives the exposed film, is detachable and can be carried into the dark room when film is to be developed.

The unexposed film is stored on a drum, from which it travels over two guides past the horizontal slit where it is exposed. It then

passes between two rollers, one the driving roller, and up through a slot into the upper removable part of the camera. The driving roller is made of a series of rubber disks mounted on a shaft and ground to size and the free roller is of brass. A Telechron clock motor drives the roller through a pair of interchangeable gears. Although the writers have always had a distaste for friction drives, this method was tried because of its simplicity, and thus far no irregularity has appeared in the records.

The slot through which the film leaves the lower part of the camera is held open only when the upper box is in place. When the box is removed, two springs automatically close the opening and thus prevent light from entering and fogging the unexposed film. The opening in the upper box is closed by a slide having a sharpened edge, so that when the slide is closed, film that has been fed into the box is cut off at the proper place.

A 3-cm focus cylindrical lens mounted in front of the horizontal slit concentrates the light in the slit image received from the radiometer mirror.

#### ACCESSORY PARTS

One must of course have a light-source for recording, and a reasonably constant source for the microphotometer. For the latter, 75-watt single helix "Street Lights" have been found very satisfactory. When run at 7.5 amp., instead of their rated 6.25 amp., they have a very high intrinsic brilliancy and their life is not unduly short.

When fine detail is being studied, a second slit is necessary to eliminate light scattered in the emulsion and elsewhere. This is placed on a stand between the plate carriage and the radiometer and adjusted to let through only that light coming from the intensely illuminated part of the emulsion.

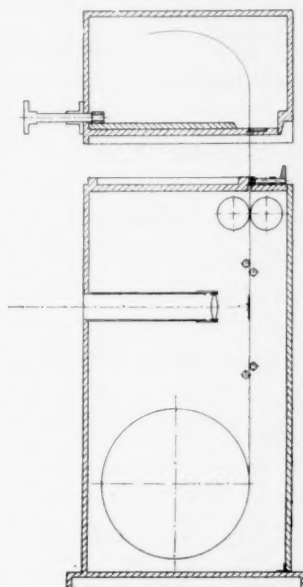


FIG. 3.—Recording film camera showing the removable part detached.

## OPERATION

The operation of the instrument is as follows: The plate is mounted in position and oriented by releasing the plate carriage and running it rapidly back and forth, at the same time shifting the plate until the slit image travels approximately parallel to the spectrum. An auxiliary eyepiece and  $45^\circ$  mirror mounted on a vertical stand are then placed in the light-beam behind the plate carriage. This eyepiece and the second microscope objective together serve as an observing microscope which enables one to make sure that the slit image is accurately focused on the photographic plate. By using the tangent screw it is then a matter of only a minute or so to attain accurate parallelism between the spectrum and the line of travel of the slit image on the plate. The lining-up is now completed by rotating the slit, if necessary, until its image is parallel to the lines in the comparison spectrum. This can be done with considerable accuracy, as the plate is viewed under a rather high magnification. The entire job of adjusting a plate on the machine takes only three or four minutes at most.

The sensitivity of the radiometer is such as to permit the use of a very narrow slit. Slit widths of the order of 0.05 mm, reduced to 0.005 mm on the plate, are ordinarily found to give ample deflections, even on spectra less than 0.5 mm in width. The effective slit width will, however, somewhat exceed the actual value, since the radiometer is sensitive to all wave-lengths and the lens system is not achromatic for the entire spectrum. In practice, the lenses are focused for maximum deflection, which will give a minimum for the effective slit width.

No very critical tests of the machine have yet been made. Perhaps the best thus far is that afforded by several cases of runs made in duplicate (in particular on hydrogen lines in early-type stars). When superposed, the tracings show exactly the same features down to the fine detail of the plate grain. It seems unlikely that such agreement could be obtained if there were any serious error in the driving mechanism.

At present two speeds for the plate drive and one for the camera are available. For most purposes the fast speed is used. This moves the plate past the slit image at a speed of about 1 mm in 80 seconds



and gives a magnification of 138:1 on the film. The other gear arrangement gives a speed one-fourth as great and consequently a magnification of 552:1.

It is often convenient to use deflections from the continuous background to the center of a line such that the dark-clear film deflection exceeds the 70 mm available on the film. Since part of the registering beam is intercepted by a mirror and brought to a focus on a transparent scale, the clear film deflections can be read visually. Considerable time can be saved by also reading the standard area deflections visually. The relation between scale readings and deflections on the recording film can be determined by noting the scale reading, say at the beginning of a run.

Some typical records are shown in Plate XII *b, c, d*. A tracing of  $H\gamma$  in  $\alpha$  Andromedae made from an 18-inch camera plate is shown in Plate XII *b*. The  $D_1$ ,  $D_2$ , and  $D_3$  lines in the star H.D. 14143 are shown in Plate XII *c* made with the fast speed. The spectrum was taken with the 18-inch camera attached to the 60-inch telescope, the dispersion at D being about 100 Å per millimeter. Since the star is of type B, the  $Na$  lines are doubtless of interstellar origin. Plate XII *d* shows a run with the slow speed on an Abbe test plate by Zeiss, consisting of a series of alternate clear and opaque spaces about 0.025 mm wide, cut in a deposit of silver. The lack of perfectly sharp corners in the tracing is probably due to the non-achromatic lens system, which precludes perfect focusing, although it is partly inherent in the test plate, which shows somewhat ragged edges under a microscope. A similar tracing was taken without the second slit in place, and under these circumstances the opaque strips showed on the record an apparent transmission of 30 per cent. This effect was of course due to scattered light reaching the radiometer and was eliminated when the second slit was put in place. Neither the position nor the width of this slit is at all critical.

As regards operation, the advantages of the instrument may be summarized as follows: (1) ease and speed of setting up plate, (2) rapidity of registration, (3) complete steadiness of zero-point at all times.

CARNEGIE INSTITUTION OF WASHINGTON  
MOUNT WILSON OBSERVATORY  
April 1932

## WIDTH OF THE D LINES OF SODIUM IN ABSORPTION<sup>1</sup>

By S. A. KORFF<sup>2</sup>

### ABSTRACT

Spectrograms of the D lines of sodium in absorption, made with a 30-foot spectrograph, have been measured with a microphotometer. The contours are found to agree with the predictions of classical (radiation damping) theory, removing discrepancies observed in preliminary work and agreeing with Minkowsky's results. The contours show the theoretical variation of opacity with the inverse square of the wave-length distance from resonance, and the variation of width with the square root of the number of atoms in the line of sight. This work is also in agreement with the quantum mechanical theory of Weisskopf and Wigner. The experiment determines a constant  $A = 2\pi e^2 \lambda^2 / 3m^2 c^4$  and hence yields a new independent value of  $e^2/m$  of  $2.51 \pm 0.2 \times 10^8$ , compared with the accepted value  $2.512 \times 10^8$ . The effect of foreign gases on the widths was studied, yielding effective "interaction radii" of  $7 \times 10^{-8}$  cm for the *Na-He* combination and  $2 \times 10^{-7}$  for *Na-H<sub>2</sub>*. The radius for *Na-Na* interaction is found to be of the order  $10^{-6}$  cm. A 2.5-m column of low-density sodium vapor was used to give an approach to astrophysical conditions.

### INTRODUCTION

It will be remembered that the classical "radiation damping" theory<sup>3</sup> gives an expression for the widths of absorption lines in the absence of interactive effects between atoms which is in essential agreement (for resonance lines) with the quantum mechanical theory of V. Weisskopf and E. Wigner.<sup>4</sup>

In previous experimental work<sup>5</sup> on the widths of the D lines of sodium in absorption the correct theoretical contour shape was obtained, but the width was observed to be somewhat greater than theory indicated. These experiments have been repeated with improved precision and the source of the discrepancy studied in detail. The new contours are found to have the widths indicated by theory,

<sup>1</sup> Contributions from the Mount Wilson Observatory, Carnegie Institution of Washington, No. 455.

<sup>2</sup> National Research Fellow at Mount Wilson Observatory.

<sup>3</sup> H. A. Lorentz, *Proceedings of the Amsterdam Academy of Sciences*, **8**, 591, 1905; W. Voigt, *Sitzungsberichte der math.-phys. Kl. der Akademie der Wissenschaften zu München*, p. 603, 1912; J. Q. Stewart, *Astrophysical Journal*, **59**, 30, 1926, and *Journal of the Optical Society of America*, **11**, 581, 1925.

<sup>4</sup> *Zeitschrift für Physik*, **63**, 54, 1930; Weisskopf, *Annalen der Physik*, **9**, 23, 1931.

<sup>5</sup> S. A. Korff, *Physical Review*, **38**, 477, 1931.

and to be in agreement with the values obtained by R. Minkowsky,<sup>1</sup> who employed a somewhat different method.

#### EXPERIMENTAL PROCEDURE

A Philips tungsten-in-neon arc was found to be a very intense source of a continuous spectrum in the yellow. The light from this source was rendered parallel by a lens and passed through an electric furnace fitted with windows. In the center of the furnace was mounted a pyrex absorption (Fig. 1) cell into which sodium had been distilled under vacuum. The light was next focused on the slit of a 30-foot spectrograph.

In order to free the sodium from occluded gases it was found necessary to give it prolonged heat treatment. After it had been intro-

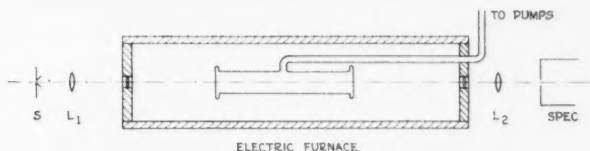


FIG. 1.—Experimental arrangement for studying the D lines in absorption

duced into a tube containing several constrictions in the form of a "sausage chain," the system was evacuated and the pumps henceforth kept running. The sodium was then driven with a flame through the several "sausages," and these were consecutively sealed off. It was next run into a bulb over which an electric furnace was placed, and slowly heated, the temperature being raised from 100° to 400° C in the course of twenty-four hours. During this time the absorption cell was baked out. The sodium was then distilled into the absorption cell for the experiment.

The temperature was determined by a mercury thermometer of the 3-inch immersion type certified by the Bureau of Standards. A chromel-alumel thermocouple reading on a galvanometer through a null bridge circuit was also used as a check.

The method used in sealing the end windows on the absorption cells was a modification of that described by C. C. Fairchild.<sup>2</sup> A

<sup>1</sup> *Zeitschrift für Physik*, **36**, 839, 1926, and **55**, 16, 1929.

<sup>2</sup> *Journal of the Optical Society of America*, **4**, 496, 1920.

pyrex tube was flared at the ends and ground flat. Upon this was laid for the end window a flat piece of pyrex, which had been cut to fit and its edges ground to a bevel (Fig. 2). Both tube and window were lowered into an electric furnace and brought up to a temperature of about  $500^{\circ}\text{C}$ . A fine oxygen flame was played on the outer edge through a hole in the furnace, thus sealing the flat to the tube at the thinnest point. The tube was left at the high temperature for half an hour to permit all strains to be dissipated in the semiplastic glass and then slowly cooled to room temperature. Very good flat end windows could thus be obtained, and with a little care no pinholes need be left in the seal. The advantages of an all-pyrex cell are

#### ABSORPTION CELL END WINDOW

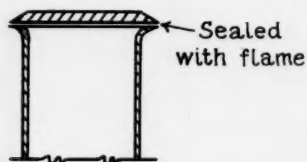


FIG. 2.—Method of sealing on end windows.

obvious, since most sealing compounds either will not stand the heat or are attacked by hot sodium vapor.

Two different lengths of tube were used, one of 24.5 cm and the other of 237.6 cm. The furnace for the long tube consisted of a 10-foot piece of asbestos-covered steel pipe on which resistance wire had been wound. The purpose of the long tube was twofold: (a) to permit lower temperatures to be used to obtain a given number of atoms in the line of sight, hence reducing the action of the sodium on the glass, and (b) to give a closer approach to astrophysical conditions and to minimize interaction between sodium atoms. The tube used was some 2.5 times longer than those Minkowsky<sup>1</sup> and others employed in studying line width, magnetic rotation, and other phenomena in sodium vapor.

The spectrograph was the 30-foot Littrow instrument in the Pasadena laboratory of the Mount Wilson Observatory, fitted with an 8-inch Michelson grating which was operated in the second order, giving a dispersion of 0.9 Å per millimeter and a theoretical resolving power of 190,000. In order to assure accurate definition of the absorption lines a number of precautions must be taken, beyond those necessary in obtaining sharp emission lines. Black cardboard dia-

<sup>1</sup> *Loc. cit.*

phragms were arranged to catch the central image and unused orders and prevent them from being scattered about the spectrograph pit. Diaphragms were also introduced into the instrument at several points to prevent any light scattered by the sides of the grating-mount from reaching the plate. Imperfectly ruled portions of the grating were of course stopped off; stops were also arranged to catch the front-and-back-surface reflections from the lens. The axis of the lens was accurately located midway between the slit and plate. The lens itself (by Brashear) had previously been tested by Mr. H. D. Babcock and found to have a good figure. The slit was set to a width of 0.03 mm and was always used at minimum length (about 1 cm) to prevent unnecessary light from entering the spectrograph. Diaphragms were also placed just before the plate-holder in order that only the portion of the plate being exposed might receive light from the pit. A Wratten filter (No. 8) cutting at  $\lambda$  4700 was used to eliminate overlapping higher orders. The methods of estimating the magnitude of the various optical sources of error are described in a previous work.<sup>1</sup>

A run was also made with the 75-foot Mount Wilson spectrograph, which employed a  $6\frac{1}{2}$ -inch Michelson grating of good quality and gave a dispersion of 0.34 Å per millimeter. The large scale given by this instrument greatly reduces all the optical errors, but the slow speed ( $f=150$ ) necessitates very long exposures, thus increasing the difficulty of accurate temperature control. The chief gain was in a demonstrable reproducibility of the widths of the lines with a different spectrograph, grating, and vacuum system.

The plates were calibrated with the aid of a step-slit raster having a range of 16 to 1, which consisted of a thin metal plate with a vertical series of rectangular apertures of constant width, each having one-half the length of the one above it. The raster, illuminated by diffuse white light, was placed over the opened slit of the spectrograph, thus producing on the plate a set of intensity marks in the form of strips with intensities proportional to the apertures. Calibrations were therefore made with the same spectrograph as was used to obtain the lines; and since the spectral region could be located with precision on the strips, the photometry was rendered monochromatic

<sup>1</sup> *Op. cit.*



within 6 Å. Ilford special rapid panchromatic plates were used and developed for five minutes in X-ray (hydroquinone) developer. These plates have high and uniform sensitivity in the yellow.

Traces of both the lines and the calibration strips were made by Miss Ware on the Koch microphotometer. The microphotometer deflections were then plotted against wave-length for the lines and against the logarithm of the intensity for the strips. The absolute contour in terms of intensity transmitted by the sodium vapor against wave-length is obviously obtained at once from these curves.

#### REDUCTION OF OBSERVATIONS

The observations thus obtained were reduced in the manner previously described.<sup>1</sup> The value of  $n$ , the number of sodium atoms per cubic centimeter, is obtained from the vapor-pressure data of Edmondson and Egerton.<sup>2</sup> This is multiplied by  $Z$ , the length of tube, and by the oscillator strength  $f$  to obtain  $N$ , the number of atoms in the line of sight.

The transmission of the sodium vapor is given by the relation  $I/I_0 = e^{-Kz}$ , where  $I_0$  is the incident intensity,  $I$  the transmitted intensity,  $K$  the opacity coefficient,  $Z$  the length of the column, and  $e$  the base of natural logarithms. The value of  $K$  is taken from Rayleigh's formula, the deduction being given in my previous paper,<sup>3</sup> in which equation (4) expresses the relation between  $K$  and the line width, namely,

$$\log (I/I_0) = AN/(\Delta\lambda)^2, \quad (1)$$

where  $A$  is a constant equal to  $2\pi e^4 \lambda^2 / 3m^2 c^4$ , the theoretical value of which is  $5.79 \times 10^{-34}$ ;  $N$  is the number of atoms  $nzf$  in the line of sight; and  $\Delta\lambda$  the wave-length distance from resonance to a point where light of intensity  $I$  has been transmitted.

#### RESULTS

The microphotometer contours give directly values of  $I$  and  $I_0$ , the latter being the intensity of the continuous background. The

<sup>1</sup> *Ibid.*

<sup>2</sup> *Proceedings of the Royal Society of London, A*, **113**, 530, 1927; H. Rowe, *Philosophical Magazine*, **3**, 538, 1927; Rodebush and Walters, *Journal of the American Chemical Society*, **52**, 2654, 1930.

<sup>3</sup> *Op. cit.*

contours also yield directly  $\Delta\lambda$ , the wave-length distance from resonance to points of intensity  $I$ . Since  $N$  is obtained from the vapor pressures as previously described, equation (1) provides a means for determining  $A$ . A set of 24 measurements for  $I/I_0 = 0.75$  and for values of  $N$  ranging from  $10^{14}$  to  $5 \times 10^{15}$  atoms, and of  $\Delta\lambda$  ranging from 0.04 to 0.2 Å, yielded for  $A$  the value  $(7.5 \pm 0.7) \times 10^{-34}$ . Further, 13 measurements for  $I/I_0 = 0.50$  gave  $A = (5.9 \pm 0.5) \times 10^{-34}$ . The practical limits in measuring the widths are represented by (a) the upper limit, which is reached when interaction-broadening sets in at high concentrations of sodium, and (b) the lower limit, which is reached when the lines become so narrow that they are not entirely resolved, in which case, as Minikowsky pointed out, they are again measured too wide. If two values of  $A$  obtained from narrow lines on the border of the incompletely resolved widths are rejected from the first set, we obtain from the remaining 22 the mean  $(5.6 \pm 0.5) \times 10^{-34}$ , and for the combined mean of all observations  $(5.77 \pm 0.5) \times 10^{-34}$ , as compared with  $5.79 \times 10^{-34}$ , the theoretical value of  $A$ . The close agreement between the values of  $A$  for  $I/I_0 = 0.75$  and 0.50 shows that  $A$  is independent of  $I/I_0$ , in agreement with equation (1).

If  $\Delta\lambda$  is plotted against  $N$  (on a double logarithmic scale) the theory yields a straight line. Figure 3 shows the experimental results, plotted as circles for the short tube and crosses for the long tube, and the theoretical line. The departures of the circles from the linear form are noted at an  $N$  of about  $2 \times 10^{15}$ . For higher values of  $N$  the lines are broadened by interaction. The usefulness of the long tube is here demonstrated, since larger values of  $N$  may thus

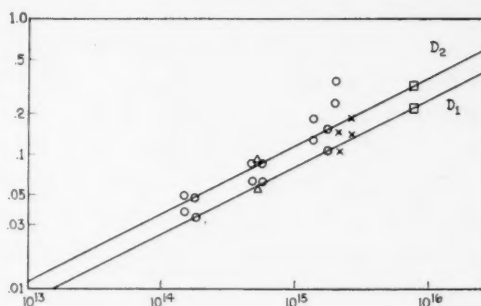


FIG. 3.—Relation between width of sodium lines  $D_1$  and  $D_2$  and effective number of absorbing atoms in the line of sight. The departure of the observed points from the theoretical line indicates interaction-broadening.



be obtained without the necessity of raising the vapor pressure to the point where interaction sets in.

The effective "interaction radius" of the  $Na$ - $Na$  combination may be calculated from the curve (Fig. 3). It appears that interaction sets in at about  $N = 1.5 \times 10^{15}$  atoms;  $z$  being 24.5 cm,  $n = 6.1 \times 10^{13}$  per cubic centimeter. The mean free time between collisions is  $t = l/v$  where  $l$  is the mean free path, given by  $l = 1/n\pi r^2$  approximately, and  $v = \sqrt{3kT/m}$  is the mean velocity of thermal motion, where  $T$  is the absolute temperature (here about  $600^\circ \text{K}$ ),  $k$  the Boltzmann constant, and  $m$  the mass of the sodium atom. Hence we can solve for  $r^2$  if we know  $t$ . For a collision or an approach to be effective in widening the line, it must occur within the lifetime of the excited state, which for the 2P state of sodium is known<sup>1</sup> to be of the order of  $1.5 \times 10^{-8}$  sec.; consequently, we obtain  $r = 2.1 \times 10^{-6}$  cm.

Since  $A$  in equation (1) involves  $(e^2/m)^2$ ,  $c^4$ , and  $\lambda^2$ , it yields on the basis of classical theory and the accepted values of  $c$  and  $\lambda$  an independent value for  $e^2/m$ . For the observed value  $A = 5.77 \times 10^{-34}$ , we obtain  $e^2/m = (2.51 \pm 0.2) \times 10^8$ , as compared with the accepted value  $2.512 \times 10^8$  (Birge).

#### WIDENING DUE TO FOREIGN GAS

The absorption cell was next so arranged that foreign gas could be admitted from a "dosing chamber" in controllable amounts. First helium was admitted. The temperature of the furnace and hence the amount of sodium vapor being kept constant, it was found that collision broadening due to helium set in when the helium pressure had reached 0.8 mm  $Hg$ . This is in good agreement with the value found in my previous work<sup>2</sup> for argon. Hydrogen was next admitted and found to start the broadening at 0.08 mm. Hydrogen is thus far more effective than helium in broadening the line. In this fact may be found the probable explanation of the anomalous widths of the D lines previously observed by the author<sup>3</sup> and also noted by G. R. Harrison<sup>4</sup> and others. A small amount of hydrogen naturally present in commercial sodium, if not carefully removed by

<sup>1</sup> A. Ellett, *Journal of the Optical Society of America*, **10**, 427, 1925.

<sup>2</sup> *Op. cit.*

<sup>3</sup> *Ibid.*

<sup>4</sup> *Physical Review*, **26**, 176, 1925.

prolonged degassing, tends to broaden the lines very considerably. Figure 4 shows the pressure-broadening curves for *He*, plotted as widths against pressures of foreign gas. The amount of sodium was kept constant at about  $2 \times 10^{13}$  atoms per cubic centimeter.

Following the argument for the interaction radius previously outlined, we obtain for the *Na-He* combination  $7.0 \times 10^{-8}$  cm, and for *Na-H<sub>2</sub>* about  $2.2 \times 10^{-7}$  cm. The physical interpretation of these values is not that of a "collision radius," but is rather in this sense: If a helium atom comes within  $7.0 \times 10^{-8}$  cm of a sodium atom while it is absorbing energy from the incident light-beam, the interaction

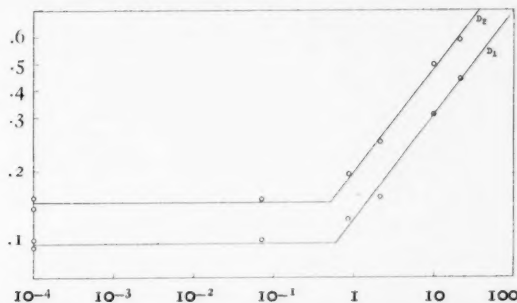


FIG. 4.—Broadening of the D lines by helium. Vertical divisions: line width in angstrom units; horizontal divisions: pressure, mm helium.

of their respective fields will suffice slightly to perturb the frequency absorbed.

While these radii may seem large, it will be recalled that the experiments on the quenching of resonance radiation yield similar values. For example, Mannkopf<sup>1</sup> found that *Na* resonance radiation was 50 per cent quenched by about 2 mm of *H<sub>2</sub>*, and Winans also finds radii several times the "gas-kinetic" value in similar experiments. The larger radius for the *Na-Na* interaction is to be expected, since this is a resonance phenomenon.

#### CENTRAL INTENSITY OF THE D LINES

A spectrogram was taken in which the exposure time was so adjusted that the intensity at the central portion of the absorption line fell on a sensitive part of the characteristic curve of the plate.

<sup>1</sup> *Zeitschrift für Physik*, **36**, 315, 1926; J. G. Winans, *ibid.*, **60**, 631, 1930.

By this means it was found that  $12 \pm 3$  per cent of the light of the continuous background was transmitted at the center of the line. The lines observed were 0.135 and 0.190 Å wide at the point where  $I/I_0$  was 0.50, and consequently were fully resolved. This residual intensity presumably represents a measure of the stray light scattered along the spectrum by faint Lyman ghosts, dust on the grating and lens, and other causes. The theoretical central intensity of the contour is practically zero.

#### SOURCES OF ERROR

The greatest source of error in the foregoing determination of  $\lambda$  lies in the photographic photometry. With the improvements in photocells it should be possible in the not too distant future to perform the experiment with a movable cell replacing the photographic plate, thus eliminating the troubles that photographic processes necessarily entail. A considerable increase in accuracy should result.

The optical sources of error have been discussed in detail in this and in previous work. It suffices to say that with a good spectrograph and ghost-free grating these errors can be made small. A monochromator in front of the spectrograph, passing only about 10 Å in the vicinity of the D lines, will materially reduce scattered light.

Accurate control of the temperature of the sodium vapor may be obtained by using long furnaces of high heat capacity, with asbestos baffles to minimize convection currents. The temperature can be measured and kept within half a degree for considerable periods, and the errors reduced to those of the vapor-pressure determinations. At the low temperatures necessary to avoid interaction-broadening, the glass is not attacked very rapidly by sodium—at 250° C a tube 25 cm in length will give lines about 0.1 Å wide at  $I/I_0 = 0.75$  and will last for some hours.

Good vacuum technique is essential, and the sodium must be thoroughly degassed to eliminate widening of the D lines by foreign gas. Degassing is accomplished by a prolonged heating of the sodium while baking out the absorption cell, as mentioned above.

It is hoped that when direct photoelectric energy-measurements

become feasible, this experiment may be repeated with increased accuracy and a better determination of  $e^2/m$ .

#### ASTROPHYSICAL SIGNIFICANCE

In astrophysics these results apply especially to the quantitative analysis of stellar, solar, and planetary atmospheres, and of such interstellar substances as have absorption lines in available spectral regions. By measuring the widths of the lines we can obtain  $N$  or  $n\lambda f$  from equation (1). Such analyses have been made by H. N. Russell<sup>1</sup> and by A. Unsöld.<sup>2</sup>

The underlying assumption is that radiation damping is the only cause of the width of the lines. This is presumed to be the case since the pressures in the reversing layer are very low. It is doubtful, however, whether radiation damping alone will fully account for the formation of all the Fraunhofer lines; presumably some other physical processes are also at work here. It is proposed to investigate this point further.

The author wishes to thank Dr. W. S. Adams, director, and Dr. A. S. King for putting at his disposal the facilities of the laboratory, and Dr. Sinclair Smith and Dr. Theodore Dunham, Jr., for helpful advice on laboratory technique and photographic photometry, respectively. Thanks are also due to Miss L. Ware for making the microphotometer tracings of the lines. He is indebted to the National Research Council for the grant of a fellowship to carry out this work.

CARNEGIE INSTITUTION OF WASHINGTON  
MOUNT WILSON OBSERVATORY  
April 1932

<sup>1</sup> *Mt. Wilson Contr.*, No. 383; *Astrophysical Journal*, **70**, 63, 1929.

<sup>2</sup> *Zeitschrift für Physik*, **44**, 796, 1927.

## THE APPLICATION OF UNSÖLD'S CHROMOSPHERIC THEORY TO THE BALMER LINES

By PHILIP C. KEENAN

### ABSTRACT

Photometric observations in the chromosphere outside of eclipse, previously carried out for  $H\beta$ , have been extended to  $H\alpha$ , giving the variation in width with height. The breadth of  $H\alpha$  decreases more rapidly than that of  $H\beta$ .

Theoretical contours computed by Unsöld's equation for a height of 300 km give relative widths of the two lines in fair agreement with the observations, and indicate that self-reversal in the chromosphere should be inappreciable in the higher lines of the Balmer series.

The preliminary photometric data on the chromospheric emission line  $H\beta$ , obtained from photographs taken outside of eclipse, and discussed in an earlier paper,<sup>1</sup> indicated that the observational quantity least affected by the numerous atmospheric sources of error was the width of the line, considered as a function of height in the chromosphere. It is further apparent that the relative widths of two lines differing not too greatly in intensity can also be fairly well determined at a given height. For this reason the observations have been extended to  $H\alpha$  to provide a check on Unsöld's theory of the formation of emission lines in the chromosphere.

The observational procedure was similar to that followed before except that Wratten panchromatic plates were used with a Wratten No. 22 orange filter placed a short distance inside the focus of the camera lens of the Rumford spectroheliograph. The dispersion was nearly the same, 3 Å/mm, for both lines, but because of the greater trouble from instrumental scattered light and the poorer photographic definition in the red region of the spectrum, the intensities of  $H\alpha$  were not as well determined as those of  $H\beta$ . For this reason only the widths of the line will be considered in this paper.

The breadths of  $H\alpha$  and of  $H\beta$ , measured at half of the maximum intensity of the line when corrected for scintillation, are plotted against height in Figure 1. The values for  $H\beta$  are taken from the earlier paper, while in the case of  $H\alpha$ , the measures were made on four exposures of the north limb of the sun taken on November 13 and 18, 1931. Plates taken on several other days show no striking

<sup>1</sup> *Astrophysical Journal*, **75**, 277, 1932.

differences in the appearance of the line, so the data are representative of the normal chromosphere.

The mean values for the two lines, indicated roughly by the dotted curves, are appreciably different in their behavior.  $H\alpha$  falls off almost linearly in width up to the highest observed altitudes, the decrease in the first 2000 km being about 20 per cent. The much slower rate of decrease for  $H\beta$  has been noted previously. The discrepancy appears to be real, although its magnitude is somewhat uncertain because of the spread of the plotted points.

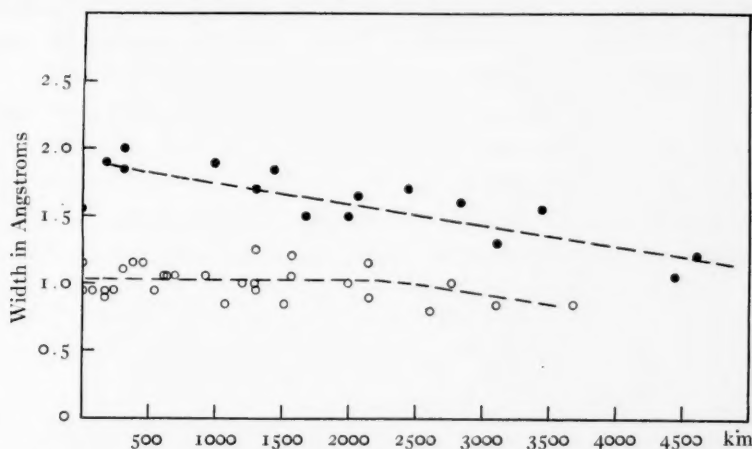


FIG. 1.—Widths as function of height in the chromosphere. The measures for  $H\alpha$  are represented by solid circles; those for  $H\beta$  by hollow circles.

Unsöld's formula for intensities<sup>1</sup> cannot be applied at present to give a predicted function for the widths, since the theoretical contour depends upon the value of the coefficient of absorption, which, as Unsöld has shown in connection with the H and K lines of calcium, probably diminishes with increasing height.

It is possible, however, to compute the relative widths of the two lines at a fixed height, which we shall take, for convenience, as 300 km. For this purpose the formula may be written

$$I = \frac{J_0}{1+sH} \left\{ 1 - \frac{3}{2Rs} + 3\sqrt{\frac{y}{2R}} - e^{-2s\sqrt{2Ry}} \left( 1 - \frac{3}{2Rs} - 3\sqrt{\frac{y}{2R}} \right) \right\} \quad (1)$$

where the notation is the same as in the previous paper.

<sup>1</sup> *Ibid.*, 69, 209, 1929.



The coefficient of absorption,  $s$ , is given by

$$s = \frac{V \pi e^2 \lambda_0^2 N f}{m c^2 \Delta \lambda_0} e^{-\left(\frac{\Delta \lambda}{\Delta \lambda_0}\right)^2} \quad (2)$$

or

$$s = s_0 e^{-\left(\frac{\Delta \lambda}{\Delta \lambda_0}\right)^2} \quad (3)$$

on the assumption of Doppler broadening.

In comparing two lines of the same series,  $\lambda_0$  and  $f$  will be the only variable factors in  $s_0$ , so we may write

$$\frac{s'_0}{s_0} = \frac{\lambda'_0 f'}{\lambda_0 f} \quad (4)$$

since  $\Delta \lambda_0$  is directly proportional to  $\lambda_0$ .

Letting the primed symbols refer to  $H\alpha$ , and using the values of the relative oscillator strengths, computed by Y. Sugiura,<sup>1</sup> we have

$$f' = 0.64, \quad f = 0.12$$

and

$$s'_0 = 7.2 s_0.$$

In the work on  $H\beta$  it was found that the observed contour at 300 km could be fitted satisfactorily by the theoretical when  $s_0$  was taken as  $12 \times 10^{-10}$ . Hence

$$s'_0 = 87 \times 10^{-10}.$$

Direct computation of the intensities across the lines by means of equation (1) gives

$$\frac{\text{Width of } H\alpha \text{ at half-maximum intensity}}{\text{Width of } H\beta \text{ at half-maximum intensity}} = \frac{0.77}{0.46} = 1.7.$$

The observed ratio, as read from the diagram, is 1.8, in satisfactory agreement with the theory.

<sup>1</sup> Scientific Papers of the Institute of Physical and Chemical Research, Tokyo, 11, 1, 1929.



The computations were carried out with the  $\Delta\lambda_0$  corresponding to a mean velocity of turbulence in the chromosphere of 15 km/sec., the value adopted by Unsöld. It may easily be verified that in a Doppler broadening formula of the type of (3) the coefficient of absorption is falling off so rapidly for a  $\Delta\lambda$  of 1 Å that a line having a total width much greater than 2 Å is practically impossible even with a great increase in  $s_0$ . Since this limiting width is quite sensitive to changes in  $\Delta\lambda_0$ , the fact that none of the chromospheric lines exceeds this limit is strong evidence that none of the elements abundant in the chromosphere is characterized by a much greater degree of turbulence.

The calculations may be extended without difficulty to  $H\gamma$ , for which  $f=0.045$ . The essential features of the theoretical contours of the three lines are given in the accompanying table, in which intensities are expressed in terms of the central intensity for the same line. The three columns give, in turn, the absorption coefficient at the center of the line, the distance of the point of maximum intensity from the center, and the maximum intensity.

THEORETICAL CONTOURS OF THE BALMER  
LINES AT A HEIGHT OF 300 KM

| Line            | $s$                   | $\Delta\lambda_{\max}$ | $I_{\max}$ |
|-----------------|-----------------------|------------------------|------------|
| $H\alpha$ ..... | $87 \times 10^{-10}$  | 0.65 Å                 | 6.5        |
| $H\beta$ .....  | $12 \times 10^{-10}$  | .3                     | 1.6        |
| $H\gamma$ ..... | $4.0 \times 10^{-10}$ | 0.2                    | 1.09       |

It is at once evident from the rapidity with which the emission peaks diminish in strength and draw together in passing toward higher lines in the series that the Balmer lines to the violet of  $H\gamma$  should show practically no self-reversal in the chromosphere. This conclusion would remain valid even if it were found necessary to change the magnitude of  $s_0$  for the stronger lines by a considerable amount, since it rests primarily upon the rate of change of  $f$  with terms in the series.

The difficulty of separating true self-reversal in narrow lines from the absorption due to scintillation and scattering in the earth's

atmosphere precludes a test of this prediction of the theory by observations made outside of eclipse. On the other hand, existing flash spectrograms, most of them taken with slitless prismatic cameras, throw little light on this point, and it remains for future eclipse observations, made with a slit spectrograph, to settle the question.

YERKES OBSERVATORY  
January 19, 1932

## THE EXCITATION OF HELIUM IN THE CHROMOSPHERE

By PHILIP C. KEENAN

### ABSTRACT

The observed *turbulent motion* of the chromospheric gases may provide the *atoms of calcium with velocities sufficient to excite atoms of normal helium by collisions*. Whether such encounters are as effective as direct absorptions of ultra-violet radiation in exciting the helium spectrum cannot be decided from the data available. On the basis of Unsöld's measures of the brightness of  $D_3$  in the chromosphere, the *intensity of radiation* required to produce the observed emission is estimated roughly as  $10^8$  times the amount that would be present if the sun behaved as a black body.

The difficulty in accounting for the presence of the lines of helium in the spectrum of the chromosphere lies in the relatively high energies of excitation involved in their production. The lowest excitation potential of the normal atom is 19.7 volts for the  $2^3S$ -state, while the lines  $\lambda 3203$  and  $\lambda 4686$  of  $He^+$ , both observed in the lower chromosphere, require 54 volts for excitation in addition to the ionization potential of 24.5 volts.

As a source of this energy R. W. Gurney<sup>1</sup> has suggested collisions between atoms of  $He$  and ions of  $Ca^{++}$  dropping under the attraction of gravity from the higher chromosphere. In falling distances given by the differences in the observed maximum heights of  $He$  and  $He^+$  in the undisturbed chromosphere, as compared to  $Ca^{++}$ , the ions would acquire kinetic energies agreeing fairly well with the corresponding excitation potentials, as W. Anderson has shown.<sup>2</sup>

An objection to this hypothesis has been raised by D. H. Menzel,<sup>3</sup> who pointed out that it does not explain satisfactorily the appearance of the stronger helium lines, including  $\lambda 4686$ , in high prominences. On the other hand, the fact that prominences usually have the same form when observed with lines of calcium, hydrogen, and helium, except that their extent is slightly greater in calcium light, is something in its favor.<sup>4</sup>

<sup>1</sup> *Monthly Notices of the Royal Astronomical Society*, **88**, 377, 1928.

<sup>2</sup> *Zeitschrift für Physik*, **49**, 749, 1928.

<sup>3</sup> *Publications of the Lick Observatory*, **17**, 297, 1931.

<sup>4</sup> E. Pettit, *Astrophysical Journal*, **76**, 9, 1932; E. J. Perepelkin, *Zeitschrift für Astrophysik*, **3**, 338, 1931.

Recent observations of the turbulent motions of the solar gases suggest the possibility of avoiding the difficulties involved in establishing this particular mechanism for the production of ions of high speed. A. Unsöld found that the contours of the lines H and K observed in emission at the edge of the sun were in satisfactory agreement with theory if the calcium atoms were assumed to have a mean random velocity of 15 km/sec.<sup>1</sup> More recently he has obtained a similar value for helium.<sup>2</sup> In the case of hydrogen, the motions appear to be of the same magnitude, although the evidence is not conclusive.<sup>3</sup> Thus the normal chromosphere seems to be characterized by turbulent currents with an average velocity of about 15 km/sec.

For the velocities required by thermal equilibrium at 4800° (1.7 km/sec. for calcium), the kinetic energy of any of the atoms would amount to only 0.6 volts, but at 15 km/sec. the energies are 1.2 volts for hydrogen, 4.7 volts for helium, and 47 volts for calcium. It follows that inelastic collisions with such calcium atoms may provide the energy necessary for the excitation of normal helium.

Whether such encounters occur with sufficient frequency to account for the observed intensity of emission cannot be determined definitely now because of the many uncertain factors involved.

The macroscopic appearance of turbulence is probably due in reality to motion in continuously shifting streams or currents of which the dimensions may vary within wide limits. Within these streams the random velocities may be expected to approximate those given by kinetic theory for the observed temperature. In thermal equilibrium the number of collisions per cubic centimeter per second between helium and calcium atoms would be about  $4 \times 10^6$ , if the pressure of calcium is taken as  $10^{-12}$  atmospheres,<sup>4</sup> and the abundance by volume of calcium with respect to helium as 1 to 1000. This estimate is, however, of little significance in connection with the number of encounters involving the high velocities of the streams, which will clearly be less if the currents comprise large masses of gas than if they are small and rapidly shifting. The variation in the proportion

<sup>1</sup> *Astrophysical Journal*, **69**, 209, 1929.

<sup>2</sup> *Zeitschrift für Astrophysik*, **3**, 77, 1931.

<sup>3</sup> Keenan, *Astrophysical Journal*, **75**, 277, 1932; **76**, 134, 1932.

<sup>4</sup> Cf. Menzel, *Monthly Notices of the Royal Astronomical Society*, **91**, 628, 1931.

of inelastic to elastic collisions with the speed of the impinging atoms in the neighborhood of the critical velocity is also an important factor. In general, we can conclude only that collisions, even in the higher chromosphere, are not necessarily so rare as to be negligible. A relatively small number of collisions may suffice to preserve the necessary concentration of excited atoms, since an atom once excited to the metastable  $2^3S$ -state will probably be raised to higher levels by absorption of radiation many times before being knocked back to the  $1S$ -level by superelastic encounters.

A rough idea of the frequency of emissions may be gained from the observed intensity of  $\lambda$  5876 ( $D_3$ ). From the measures of Unsöld,<sup>1</sup>  $D_3$  in the middle chromosphere can be taken as a line with an effective width of  $0.5 \text{ \AA}$  and an intensity  $0.03$  that of the continuous spectrum at the center of the disk. By Planck's law the energy radiated by  $1 \text{ cm}^2$  of the photosphere at this wave-length is  $8.0 \times 10^6$  ergs per second per angstrom. Hence, the intensity of the radiation from the chromosphere is

$$\frac{8.0 \times 10^6 \times 0.03 \times 0.5}{\pi} = \frac{1.2 \times 10^5}{\pi}.$$

If the helium chromosphere is considered as a sheet of uniform density having a thickness of  $5000 \text{ km}$ , as is justifiable for a first approximation in this case because of the slow decrease in the brightness of  $D_3$  with increasing height, the intensity at a height of  $1000 \text{ km}$  above the photosphere is produced by a column of gas  $1.5 \times 10^{10} \text{ cm}$  in length. Disregarding self-absorption, and taking the emission as constant throughout this column, we obtain for  $i$ , the average intensity due to a cubic centimeter of gas, the value

$$\frac{8.0 \times 10^{-6}}{\pi}.$$

The total energy radiated per cubic centimeter is

$$4\pi i = 3.2 \times 10^{-5} \text{ ergs per second,} \\ = nh\nu,$$

<sup>1</sup> *Zeitschrift für Astrophysik*, **3**, 77, 1931.

where  $n$  is the number of transitions giving rise to the line. Solving for  $n$ , we obtain finally

$$n = 10^7 \text{ transitions per cubic centimeter per second.}$$

To obtain the corresponding number of excitations it would be necessary to introduce the factors for the fraction of atoms in the normal state, self-absorption, and the ratio of the number of  $2^3P-3^3D$  transitions to the total number, and this cannot be done in the present state of our knowledge. However, the value of  $n$  at least suggests the order of magnitude of the excitations. On this basis we can make a provisional estimate of the intensity of solar radiation that would be required to produce excitation through direct absorption by helium atoms in the normal state. This alternative means of excitation is favored by Menzel<sup>1</sup> as the source of the necessary energy.

The longest wave-length that can be absorbed by the neutral atom is 584 Å. From the discussion given by Gurney,<sup>2</sup> it may be seen that, since an ionized calcium atom probably makes not less than  $10^3$  absorptions per second, and since the ratio of the number of quanta at 584 Å to the number at 3969 Å, calculated from Planck's formula, is  $10^{-13}$ , the solar radiation in the ultra-violet must be in excess of that from a black body by a factor of about  $10^8$  if the absorptions are to be as numerous as the observed emissions of  $D_3$ . The assumption is made that the absorption coefficients of helium are not greatly different from those of ionized calcium.

While collisional excitation is effective only on the sun itself, such a large excess of ultra-violet radiation would have a wider influence. To explain terrestrial magnetic storms and auroras, Maris and Hulburt<sup>3</sup> have supported the hypothesis that the sun experiences local outbursts of ultra-violet emission giving rise to flares of radiation in which the intensity between  $\lambda$  500 and  $\lambda$  1000 Å has  $10^5$  times the black-body value. They have suggested that these flares may be responsible also for the rapid changes in cometary spectra,<sup>4</sup> and

<sup>1</sup> *Publications of the Lick Observatory*, **17**, 297, 1931.

<sup>2</sup> *Op. cit.*

<sup>3</sup> *Physical Review*, **33**, 412, 1929.

<sup>4</sup> *Ibid.*, p. 1046, 1929.



N. T. Bobrovnikoff<sup>1</sup> has concluded that the light of comets is excited chiefly by ultra-violet radiation from the sun.

From these several effects it should eventually be possible to make independent estimates of the required excess of radiation, the consistency of which may permit us to decide whether collisions or absorptions are more important in the chromosphere.

If collisions play an important part in exciting helium in the normal chromosphere, they should be almost equally effective in prominences. According to the estimates of Pettit,<sup>2</sup> based upon the data of Pannekoek and Doorn, a typical prominence has a hydrogen content of  $2 \times 10^{13}$  atoms per cubic centimeter. Unsöld<sup>3</sup> also found that the density of both hydrogen and calcium in prominences was of the same order of magnitude as that in the chromosphere. The continuous internal agitation of the matter in prominences has been well established by the studies of Pettit, who has measured velocities up to 15 km/sec. even in quiescent prominences. Since the conditions of excitation are thus essentially the same in prominences and in the ordinary chromosphere, it is not surprising to find the helium spectrum consistently present along with H and K and the hydrogen lines.

It is difficult to find evidence bearing upon the source of excitation from the intensities of the emission lines. Disturbed areas favorable to collisions in which the relative velocities are higher than the average are usually characterized by more intense general radiation. However, the presence of collisional effects should be revealed by a marked strengthening of the helium lines when the mean velocity approaches 30-40 km/sec., since impacts between two helium atoms begin to become effective at these speeds. The lines of  $He^+$ , of which  $\lambda$  4686 alone is readily accessible to observation, deserve particular attention. Their high excitation potential should make them especially sensitive to changes in the degree of turbulence.

It is a pleasure to thank Dr. Struve and Dr. Elvey for the suggestions which they have given freely in discussions of the subject of this note.

YERKES OBSERVATORY

April 1932

<sup>1</sup> *Publications of the Lick Observatory*, **17**, 479, 1931.

<sup>2</sup> *Op. cit.*

<sup>3</sup> *Zeitschrift für Physik*, **59**, 353, 1929.

## A STUDY OF THE COMPOSITE SPECTRUM OF THE A-TYPE STAR 14 COMAE

By W. W. MORGAN

### ABSTRACT

The A5 star 14 Comae has been found to contain lines of various degrees of sharpness in its spectrum. A number of lines  $Ti\ II$  and  $Fe\ II$  are present which probably consist of a fairly narrow core directly superposed over a broad, shallow underlying line. There are also present several very broad, shallow lines most of which are near the limit of visibility. The  $Mg\ II$  line  $\lambda\ 4481$  belongs to this latter class. All the other lines of the second spectrum are probably due to  $Fe\ I$ . The radial velocities of the two sets of lines are identical, and it seems practically certain that the spectrum observed comes from one star only. A possible explanation of the origin of the spectrum somewhat similar to that found by Struve for 17 Leporis is given. The radial velocity of 14 Comae is constant.

The spectrum of 14 Comae ( $\alpha 1900 = 12^h 21^m$ ;  $\delta 1900 = +27^\circ 49'$ ; mag. = 5<sup>m</sup>15) is classed as A5 in the *Henry Draper Catalogue*. The great strength of the hydrogen lines prevents its being assigned to a later class, while the equality of  $Ca\ I\ K$  with  $H\epsilon + H$  shows that the spectrum cannot be classed earlier. In the course of an examination of Yerkes spectrograms of A-type stars several very unusual features were noticed in its spectrum. The lines of  $Ti\ II$  and  $Fe\ II$  are slightly broadened but are fairly well defined. In contrast to these lines,  $Mg\ II\ 4481$  is a very hazy, diffuse line 5A in width. I have examined spectra of the five hundred A-type stars for which spectrograms have been obtained at Yerkes and have found only one other star which possesses a faint, diffuse  $\lambda\ 4481$  when other lines in the spectrum are narrow. This star, 17 Leporis, was found to have a composite spectrum by Otto Struve several years ago and has been discussed by him.<sup>1</sup>

The plates on the basis of which the present study was made were obtained with the Bruce spectrograph attached to the forty-inch refractor. A dispersion of one prism was used which gives a scale of 30 Å per millimeter at  $\lambda\ 4500$ .

There are a number of other lines in the spectrum which resemble  $Mg\ II\ 4481$  in being very broad and shallow. All the strongest lines of  $Fe\ I$  are present as faint, hazy lines having widths of about 5 Å.

<sup>1</sup> *Astrophysical Journal*, 76, 85, 1932.

Table I gives the lines which are sensibly unblended and similar to *Mg* II 4481.

The first six lines are members of the multiplet  $a^3F - y^3F^o$  of *Fe* I. All the lines in Table I with the exception of  $\lambda$  4045 and  $\lambda$  4481 are very faint even on Process plates, and most of them cannot be seen at all on the coarser-grain Eastman-40 plates. Line 4045, the strongest of the *Fe* I lines, gives the impression of being made up of a broad, hazy line, with a faint, sharper core superposed. An examination of the stronger lines in the spectrum shows that probably all the narrower, stronger lines are superposed over the same broad

TABLE I  
BROAD, SHALLOW LINES IN SPECTRUM  
OF 14 COMAE

| $\lambda$    | Int. | Iden.        |
|--------------|------|--------------|
| 4005.1.....  | 1    | <i>Fe</i> I  |
| 4045.90..... | 3    | <i>Fe</i> I  |
| 4063.85..... | 2    | <i>Fe</i> I  |
| 4071.95..... | 1    | <i>Fe</i> I  |
| 4131.95..... | 1    | <i>Fe</i> I  |
| 4143.60..... | 2    | <i>Fe</i> I  |
| 4260.70..... | 2    | <i>Fe</i> I  |
| 4481.17..... | 3    | <i>Mg</i> II |

type of line that is shown by *Fe* I and *Mg* II. This is best shown by the lines *Sr* II 4077, *Sr* II 4215, *Fe* II 4233, *Ti* II 4468, and *Ti* II 4501.

The radial velocity of 14 Comae is constant, according to measures made at the Lick and Yerkes observatories. The velocity determined from the plates at Lick is  $-2.1$  km/sec. A value of  $-4.4$  km/sec. was found at Yerkes from measures of six plates. There is no evidence for variation in the radial velocity.

The radial velocity determined from the diffuse lines is the same as that found from the sharper lines. This makes it almost certain that we are not concerned with two bodies, but that both types of lines arise from the atmosphere of the same star. There is other evidence which makes this even more certain. At spectral type A5, *Mg* II 4481 is about as strong as any line in the spectrum of a normal star, with the exceptions, of course, of lines of hydrogen and ionized calcium. For the narrow-line spectrum to be complete, then, we

should expect a line at  $\lambda$  4481 similar in appearance and strength to  $Ti$  II 4468, 4501, 4571, and other strong lines. Instead of this, we find a decidedly fainter and far broader line which is not at all similar in appearance to the stronger ionized metallic lines. Another feature of interest is that the spectrum, if considered in the light of the diffuse lines alone, would indicate the same spectral type and temperature as that determined from the lines of  $Ca$  II,  $Ca$  I, and  $Fe$  II. I have found from an examination of the Yerkes spectra of A-type stars that  $Fe$  I 4045 becomes equal in intensity to  $Mg$  II 4481 at spectral type A<sub>3</sub> or A<sub>5</sub>. The two lines are approximately equal in 14 Comae, and this would make the spectral type of the faint spectrum the same as that found for the stronger lines.

From these considerations it seems safe to conclude that we are concerned with light coming from a single star only. This raises a serious difficulty when an explanation of the appearance of the lines is sought for. The presence of diffuse absorption lines in a stellar spectrum has been explained by Struve and Shajn<sup>1</sup> as an effect of the axial rotation of the star. If the lines are broadened by Doppler shift due to rotation, however, we should expect all of the lines in a star's spectrum to be broadened approximately to the same degree. There is no provision for the presence of both sharp and diffuse absorption lines in the same spectrum. (The broadening of the lines of hydrogen and helium due to Stark effect is not considered.) Up to the present time, the only A-type star known to have both sharp and diffuse lines in its spectrum is 17 Leporis. This star is definitely abnormal, as many of the lines in its spectrum vary in intensity and appearance. Struve has suggested an explanation of the presence of both sharp and diffuse lines in its spectrum by assuming that the broad lines originate in the reversing layer of the star itself, which is rotating at a rather high velocity, while the sharp lines are due to an outer shell of gas separated from the star. In the case of 17 Leporis the complex changes in the lines are interpreted as due to the successive shells of gas being expelled from the star and receding from it. As the lines vary little if at all in the spectrum of 14 Comae, the explanation would call for a gaseous shell which remained at about the same position with reference to the central star. If the

<sup>1</sup> *Monthly Notices of the Royal Astronomical Society*, **89**, 222, 1928.

star has a rather high speed of rotation, we should expect a spectrum similar in type to that which is actually observed in the case of 14 Comae, that is, comparatively sharp lines superposed over hazy diffuse ones.

TABLE II  
WAVE-LENGTHS OF LINES IN THE SPECTRUM OF 14 COMAE

| $\lambda$  | Int. | Iden.                                 | $\lambda$  | Int. | Iden.                                 |
|------------|------|---------------------------------------|------------|------|---------------------------------------|
| 4005.1...  | 1NN  | Fe I .25                              | 4325.90... | 2    | Sc II .00, Fe II .77                  |
| 4012.45... | 3    | Ti II .40                             | 4338.18... | 7    | Ti II 7.92                            |
| 4023.99... | 1NN  |                                       | 4340.32... | 50   | H $\gamma$ .46                        |
| 4031.05... | 2NN  |                                       | 4351.94... | 4    | Fe II .77                             |
| 4045.90... | 3NN  | Fe I .82                              | 4374.85... | 6    | Sc II .46, Ti II .82,<br>Y II .95     |
| 4054.70... | 1NN  |                                       | 4383.51... | 4    | Fe I .55                              |
| 4063.85... | 2NN  | Fe I .60                              | 4385.62... | 4    | Fe II .39                             |
| 4071.95... | 2N   | Fe I .75                              | 4395.25... | 7    | Ti II .04, Ti II .80                  |
| 4077.84... | 6    | Sr II .71                             | 4400.06... | 3    | Ti II 9.77, Sc II .38                 |
| 4101.68... | 50   | H $\delta$ .74                        | 4415.50... | 3    | Fe I .13, Sc II .55                   |
| 4131.95... | 1NN  | Fe I 2.06                             | 4417.13... | 5    | Fe II 6.81, Ti II .71                 |
| 4143.60... | 2NN  | Fe I .87                              | 4444.36... | 7    | Ti II 3.80, Ti II 4.56                |
| 4163.42... | 2    | Ti II .65                             | 4450.47... | 1    | Ti II .49                             |
| 4172.30... | 4NN  | Ti II 1.90, Fe II 3.48,<br>Ti II 4.11 | 4468.56... | 6    | Ti II .49                             |
| 4178.31... | 3N   | Y II 7.53, Fe II 8.87                 | 4481.17... | 3NN  | Mg II .23                             |
| 4196.1}    | 2NN  | Fe I 8.31, Fe I 9.10,                 | 4487.6}    | 2    | Ti II 88.32, Fe II                    |
| 4204.4}    |      | Fe I 02.03                            | 4492.0}    |      | 89.21, Fe II 91.41                    |
| 4215.63... | 7    | Sr II .52                             | 4501.52... | 5    | Ti II .27                             |
| 4226.67... | 7    | Ca I .73                              | 4508.19... | 2N   | Fe II .29                             |
| 4233.15... | 5    | Fe II .16                             | 4515.27... | 1    | Fe II .34                             |
| 4246.81... | 6    | Sc II .83                             | 4520.43... | 1    | Fe II .24                             |
| 4260.70... | 2NN  | Fe I .49                              | 4522.75... | 3    | Fe II .64                             |
| 4272.20... | 3NN  | Fe I 1.17, Fe I 1.78,<br>Fe II 3.35   | 4534.26... | 5    | Ti II 3.97, Fe II 4.17                |
| 4290.13... | 4    | Ti II .23                             | 4549.71... | 8    | Ti II .64, Fe II .48                  |
| 4294.13... | 3    | Ti II .10                             | 4563.73... | 4    | Ti II .76                             |
| 4300.31... | 6    | Ti II .05                             | 4572.06... | 6    | Ti II 1.97                            |
| 4302.40... | 2    | Ti II 1.93, Fe II 3.18                | 4583.42... | 8    | Fe II 2.84, Fe II 3.84,<br>Ti II 3.45 |
| 4307.90... | 4    | Ti II .89, Fe I .91                   | 4861.21... | 50   | H $\beta$ .33                         |
| 4313.21... | 3    | Ti II 2.88, Sc II 4.09                | 4923.8...  | 4    | Fe II .92                             |
| 4315.03... | 5    | Ti II 4.98                            | 5018.4...  | 7    | Fe II .44                             |
| 4320.87... | 2    | Ti II .95, Sc II .73                  |            |      |                                       |

On several of the best plates of 14 Comae the line Sc II 4246 is definitely narrower than other lines of the same strength which are due to Ti II, Fe II, and Ca I. The line is abnormally strong in the narrow-line spectrum and the hazy background line is either missing or very faint. If the line were weak in the reversing layer of the star and equally strong with other lines which originate in the shell, then

it would appear sharper than other lines for which there is a well-marked underlying diffuse line.

Some of the spectral lines were suspected of varying both in intensity and in appearance, but the material is not good enough to make certain. The lines are so faint that the spectrum can be adequately studied on Process plates only. As the star is too faint to obtain a series of Process plates with the Bruce spectrograph, it would probably not be possible to decide on the question of the possible variation of the lines, even if a long series of plates were available.

The wave-lengths, intensities, and identifications of all the lines in the star's spectrum which could be measured are given in Table II. The intensities are on an arbitrary scale, the faintest line discernible being recorded as intensity 1.

YERKES OBSERVATORY  
WILLIAMS BAY, WIS.  
May 11, 1932